



# OBSERVED AND FUTURE CLIMATES OF THE **TORRES STRAIT REGION**

Ramasamy Suppiah, Janice Bathols, Mark Collier,  
David Kent and Julian O'Grady



ISBN: 978-1-921826-25-2

Enquiries should be addressed to:

Dr. Ramasamy Suppiah  
CSIRO Marine and Atmospheric Research  
107 Station Street. Aspendale. VIC., 3195  
E-mail: [suppiah.ramasamy@csiro.au](mailto:suppiah.ramasamy@csiro.au)

For copies of the report, please contact

John Rainbird  
Climate Change and Coastal Coordinator  
Land and Sea Management Unit  
Torres Strait Regional Authority  
E-mail [john.rainbird@tsra.gov.au](mailto:john.rainbird@tsra.gov.au)

## **Copyright and Disclaimer**

© 2010 CSIRO To the extent permitted by law, all rights are reserved and no part of this publication covered by copyright may be reproduced or copied in any form or by any means except with the written permission of CSIRO.

## **Important Disclaimer**

CSIRO advises that the information contained in this publication comprises general statements based on scientific research. The reader is advised and needs to be aware that such information may be incomplete or unable to be used in any specific situation. No reliance or actions must therefore be made on that information without seeking prior expert professional, scientific and technical advice. To the extent permitted by law, CSIRO (including its employees and consultants) excludes all liability to any person for any consequences, including but not limited to all losses, damages, costs, expenses and any other compensation, arising directly or indirectly from using this publication (in part or in whole) and any information or material contained in it.

Cover images – TSRA



## **ACKNOWLEDGEMENTS**

The work of the authors draws upon research findings of many colleagues within CSIRO Marine and Atmospheric Research and overseas research institutions. We acknowledge the modelling groups, the Program for Climate Model Diagnosis and Intercomparison (PCMDI) and the WCRP's Working Group on Coupled Modelling for their roles in making available the WCRP CMIP3 multi-model dataset. Support of this dataset is provided by the Office of Science, US Government Department of Energy.

Liaison between CSIRO, Marine and Atmospheric Research and the Torres Strait Regional Authority has been facilitated by David Hanslow (now with Department of Environment, New South Wales) and John Rainbird from TSRA. John Rainbird and John Clarke from CSIRO provided useful comments on a draft of the report.

Dean Collins from the Australian Bureau of Meteorology and Kasis Inape from PNG National Weather Service kindly provided necessary observational data.

This work was produced by CSIRO, Marine and Atmospheric Research under the contract to the Land and Sea Management Unit of the Torres Strait Regional Authority. This work also contributes to Climate and Adaptation Flagship. Financial support from the Torres Strait Regional Authority is also acknowledged.



## EXECUTIVE SUMMARY

This report has been prepared by CSIRO Marine and Atmospheric Research for the Land and Sea Management Unit of the Torres Strait Regional Authority (TSRA). It describes the main drivers that dominate most of the observed variability and trends in climate of the past century. Climate change projections for various climate variables are produced from simulations conducted for the Fourth Assessment Report of the Intergovernmental Panel on Climate Change (IPCC), published in 2007 (IPCC, 2007).

Climate change due to the increase in greenhouse gas concentrations is now inevitable. Climate change will continue to impact until (and to a lesser known degree beyond) a stabilisation and subsequent reduction of greenhouse gas concentration in the atmosphere can be achieved. We therefore need the best possible estimates of regional climate changes and of the sensitivity of natural, economical and social sectors to such changes.

Best estimates based upon AR4 global climate models for changes and ranges of uncertainty to solar radiation, maximum, minimum and mean temperatures, mean rainfall, relative humidity, wind speed, potential evaporation and apparent temperatures are given for 2030, 2050 and 2070 for A2 and A1FI emission scenarios. Climate model simulations also indicate a range of possible changes in ENSO and tropical cyclone behaviour. It is important to recognise that the majority of Global Climate Models (GCMs) do not as yet factor in a number of major positive feedback processes, and as such model predications are likely to be conservative. In addition, with their coarse horizontal resolution, do not capture many of the details of the flow and extremes of the region. The practical implications of these projections of climate change suggest possible widespread impact across the Torres Strait Region. Such impact can significantly affect marine and terrestrial ecosystem health, agricultural productivity, water resources, fisheries, human health, tourism, and pest abundance and distribution in the region.

Of the variables modelled in this study those expected to show the most significant changes due to climate change are rainfall (increase in variability and wet season intensity), ambient and atmospheric temperature and potential evaporation.

### ***Observed climate trends in the Torres Strait region***

**Surface air temperature:** The annual average air temperature is about 26.8 °C. December is the warmest month with 28.1 °C, while August is the coolest month with 25.3 °C. Since 1960, maximum, minimum and mean temperatures at Thursday-Horn Islands show a positive trend with strong inter-annual variability. The maximum and minimum temperatures increased by 0.32 °C and 0.18 °C/per decade between 1960 and the mid 1990s. From the mid 1990s to 2009, maximum and minimum temperatures increased by 0.67 °C and 0.35 °C/per decade. The mean temperature increased by 0.25 °C/per decade between 1960 and the mid 1990s and by 0.51 °C/per decade from the mid 1990s and 2009. Since the increases in the later period were drawn from a smaller sample, caution is needed when interpreting the results.

**Sea surface temperature (SST):** The average annual SST in the region is about 28.0 °C and shows small variation throughout the year. The long-term average SST for the wet season is 28.3 °C and for the dry season is 27.4 °C. The average annual SSTs in the region have risen by about 0.16 to 0.18 °C per decade from 1950 to

present. Increases in SST can have major implications for marine ecosystems and fisheries. Whilst expected changes in SST were unable to be modelled in this study, an average increase in SST of 2 °C in tropical Australia is expected to lead to annual bleaching with 97% of reefs affected (Johnson and Marshall, 2007).

**Apparent temperature:** Apparent temperature refers to how combinations of air temperature, humidity, solar radiation and wind speed feel to humans, based on physiology and clothing. The annual apparent temperature is 38.4 °C compared to the annual air temperature of 26.8 °C. The average wet season apparent temperature is 43.8 °C and for the dry season is 33.6 °C. Higher apparent temperature is a result of high relative humidity throughout the year, more intense solar radiation and weaker winds during the wet season (and vice versa for the dry season). High apparent temperatures can also lead to health impacts such as fatigue and heat stress, particularly on the sick and aged population.

**Rainfall:** Rainfall shows strong variations on intra-seasonal to inter-decadal time scales. Wet season (October to April) rainfall dominates the variability with an average amount of 1750 mm. The dry season (May to September) receives only about 90 mm. Daily rainfall shows variability on the intra-seasonal time scale of 30-50 days, particularly during the Australian monsoon season (December to February).

**ENSO:** El Niño-Southern Oscillation (ENSO) plays a major role in influencing climate variations on inter-annual and inter-decadal time scales. A strong relationship between the Southern Oscillation Index (SOI) and rainfall shows that above-average rainfall during the wet season is associated with La Niña years, while below-average rainfall is linked to El Niño years. It is yet unclear how the frequency and variability of ENSO might affect climate change under enhanced greenhouse conditions.

**Extreme rainfall:** A distinct low pressure system forms over the Torres Strait / Coral Sea during heavy rainfall events over the Torres Strait region, Cape York and the rainforest region. Mean sea level pressure, wind and out-going long wave radiation (OLR) anomalies based on extreme rainfall events indicate that they are a part of large-scale atmospheric circulation patterns during the wet season. Higher temperatures are observed over southern Australia during heavy rainfall events in northern Australia. Heavy rainfall events and strong winds occur particularly during onset and active periods of the monsoon, affecting the coastal environment and ecosystems of the region.

**Tropical cyclones:** The direct impact of severe tropical cyclones is small, but the indirect effect of cyclones that move towards the north-east coast of Australia, particularly crossing Cape York, can be significant through storm surges generated by these storms. Ocean inundation is a common hazard affecting many communities in this region.

## **Simulating future climates of the Torres Strait region**

Probability-based climate change projections for solar radiation, temperature, apparent temperature, rainfall, relative humidity, wind speed and potential evaporation are given for SRES A2 and A1FI emission scenarios for the 50<sup>th</sup> percentile (as the best estimate) and low and high ranges are given as 10<sup>th</sup> and 90<sup>th</sup> percentiles. Upper and lower ranges in projected changes reflect model-to-model variations. Temperature and rainfall projections for 2030 do not differ much compared to northern Australia. Comparing climate change projections for the

Torres Strait region, temperature and rainfall in particular projections are very similar to those for northern Australia. Especially projections for tropical rainforest regions are very similar for 2030. However, the best estimate for 2070 is slightly higher for the Torres Strait region as we considered only two emission scenarios, A2 and A1FI.

**Solar radiation:** Decreases dominate projected changes in solar radiation. The best estimates of annual changes in solar radiation by 2030 for A2 and A1FI emission scenarios are -0.31% and -0.43%, with ranges between -1.18% and 0.82% and between -1.39% and 0.81%, respectively. Slightly higher decreases and larger ranges are projected for 2050 and 2070 for the two emission scenarios.

**Temperature:** The Torres Strait region is expected to warm in response to the increase in average global temperature. The best estimate for regional annual average temperature increase by 2030 is 0.87 °C, with a range of uncertainty of 0.62 to 1.08 °C for the A2 emission scenario. For the A1FI emission scenario the annual increase by 2030 is 1.02 °C with the range of uncertainty of 0.73 to 1.27 °C. Larger increases are projected for 2050 and 2070 for these emission scenarios.

**Apparent temperature:** The projected increase in the average annual apparent temperature for the A2 emission scenario by 2030 is 1.32 °C with a range of uncertainty of 0.87 to 1.70 °C, and for the A1FI emission scenario is 1.56 °C with a range of uncertainty of 1.03 to 1.96 °C. Best annual estimates are 2.29 and 3.24 °C for the A2 emission scenario and 2.70 and 3.82 °C for the A1FI emission scenario for 2050 and 2070. Larger increases and ranges are projected for 2050 and 2070 for these emission scenarios. Differences in projected changes among seasonal values are small. Increases in apparent temperature are larger under climate change conditions due to changes in air temperature and wind speed, as changes in relative humidity and solar radiation are small. The Queensland Heat Stress Response Plan specifies that a 'heat warning' will be declared when the ambient temperature is expected to exceed 36 °C for Brisbane for 2 days or more, and an 'extreme heat warning' will be declared when the ambient temperature is expected to exceed 40 °C for Brisbane for 2 days or more. Communities in the Torres Strait would be accustomed to higher ambient temperatures than people in Brisbane, but communities will need to consider how they might respond to predicted increases in ambient temperature, to avoid impact to health and productivity.

**Rainfall:** Projected rainfall changes include both increases and decreases, but increases dominate the overall changes. The best estimate of regional average annual rainfall change for the A2 emission scenario for 2030 is +1.24% with a range of uncertainty of -2.97 to + 5.33%. For the A1FI emission scenario the best estimate for 2030 is +1.46% with the range of uncertainty of -3.49 to +6.27%. Larger ranges and slight increases in means are projected for 2050 and 2070. Increases are relatively larger for December to February, March to May and September to November compared with June to August. An increase in rainfall intensity may increase the risk of flooding and erosion. Increased variability will have implications for food production, rainwater supplies and island ecosystems.

**Relative humidity:** Due to the location in the tropics, relative humidity is constantly high during the year in the Torres Strait region. However, changes in relative humidity in the future are projected to be less than 1% ranging between -1 and +1%.

**Wind speed:** Changes to annual wind speed are also expected to be small. The best estimate for annual wind speed change by 2030 for the A2 emission scenario is +0.34% with a range between -0.95 and 1.72%. For the A1FI emission scenario, the

annual change is +0.37% with a range between -1.12 and 2.47%. A very small increase has been projected in annual and seasonal values for 2050 and 2070 for both emission scenarios.

**Potential evaporation:** Overall there is an increase in potential evaporation in the future with the greatest increase under the A1FI emission scenario. The best estimate of annual increase by 2030 for the A2 emission scenario is 2.63% with an uncertainty range between 1.94 and 4.72%. For the A1FI emission scenario, the annual increase by 2030 is 3.74% with an uncertainty range between 2.28 and 5.87%. Larger increases and ranges are projected for 2050 and 2070. Increases in the potential evaporation may have significant implications for ground water and fresh water supplies, with consequences for both communities and island ecosystems.

**El Niño-Southern Oscillation (ENSO) phenomenon:** ENSO is the major driver of the inter-annual variability of climate of the region. The climate change assessments are based on coupled-ocean-atmosphere GCMs. Although these are state-of-the-art models it is acknowledged that they are not fully realistic. In particular, the current generation of GCMs inadequately represent variability associated with ENSO. Furthermore, there is no consensus on the simulation of likely changes in ENSO characteristics. A major task in the near future is to refine coupled-ocean atmosphere models to provide simulations of ENSO changes in which we can have confidence, and to use the models to investigate related effects including possible changes in the behaviour of tropical cyclones. Some of the developments are in progress and will be incorporated in simulations for the IPCC Fifth Assessment Report due in 2013.

**Tropical cyclones:** There is a large uncertainty about changes to tropical cyclone behaviour due to enhanced greenhouse conditions. However, a recent review of tropical cyclone characteristics simulated by models suggests an increase in globally averaged tropical cyclone intensity by 2-11% by 2100. This leads to an increase in the order of 20% for the precipitation rate within 100 km of the storm. These models also suggest a decrease in the frequency of tropical cyclones in the Southern Hemisphere with mixed changes in northern Australia. Further investigation is needed to establish the physical basis and statistical significance of these changes.

The need for developing better methods to produce improved climate change projections under enhanced greenhouse conditions is widely recognised. Some of the sensitivity studies using climate change projections to ecosystems and other sectors by colleagues at James Cook University, CSIRO Sustainable Ecosystems, and others under the Marine and Tropical Sciences Research Facility (MTRSF) suggest that enhanced greenhouse conditions can have significant impact on ecosystems, economy and tourism, human settlements, etc. Even in the absence of confident local projections of climate change, developing the ability to assess the impact of climate change on particular activities and sectors is a valuable undertaking. It will enable rapid assessments to be made of potential impacts and proposed adaptation strategies once uncertainties in the climate projections are reduced.

## Potential climate change impacts in the Torres Strait region

The changes projected by the state-of-the-art GCMs suggest there is little room for complacency when dealing with the potential impact on various sectors, despite their uncertainties. The possible small increase in rainfall, higher temperature and increased potential evaporation, and possible changes in ENSO and tropical cyclone behaviour suggest the potential for widespread impact in the region. Such impacts are likely to lead to predominantly negative consequences on the health of marine and terrestrial ecosystems, agricultural productivity, water resources, fisheries, human health, tourism, pest abundance and low lying islands. These impacts would increase in severity beyond any stabilisation in atmospheric greenhouse gas concentrations at current levels.

**Sea Level:** Increases in sea level due to climate change are expected to pose the greatest threat to the wellbeing and viability of low lying island communities. Tide gauge data from the region suggest sea level rise of 6 mm per year between 1993 and 2010, twice the global average. Whilst great caution must be used in interpreting sea level rise from tide gauges, especially over relatively short data periods, this figure is consistent with the SEAFRAME sea level gauge data recorded from Papua New Guinea of 5.9 mm per year over a similar period. This report was not able to model predicted changes in sea level for the Torres Strait region. There is still great uncertainty associated with the expected scale and timing of rises in sea level due to the highly dynamic nature of major ice sheets. The IPCC predicts up to 0.8 m sea level rise by 2100, but higher levels cannot be excluded. It is likely that increases in sea level will not be linear. Current warming of the oceans and atmosphere are likely to drive an increase in global sea level for at least several centuries, even if we drastically reduce the greenhouse gases emissions at present.

## Conclusions and recommendations

- Simulated changes in climate indicate that a significant degree of climate change in the Torres Strait region is inevitable, and likely to become increasingly apparent over the next 30-100 years. Changes are expected in both the mean values and in the magnitudes and frequencies of these extremes. Therefore long-term planning should not assume that future climate and resources will be as they were over the past 100 years. Significant adaptation to a changing climate will be required.
- Characteristics of water quality, flooding areas and storm surges could change significantly due to changes in the characteristics of climate drivers operating in the region, particularly monsoon, ENSO and tropical cyclones. Anticipated changes have significant implications for the sustainable development of planned infrastructure including coastal development, industry and bridges.
- Changes in apparent temperature could have increasing impact on human populations of the region. These changes would affect daily life, the economic livelihood of inhabitants and the ecosystem within the region. Significant changes in management may be required for adaptation strategies to ensure sustainability.
- ENSO-related climate change at decadal and century scales is expected to affect the region. Some plant and fish species may come under increasing stress, causing long-term irreversible change in species composition.

- Coastal ecosystems will be affected by rises in sea level, storm surges, and storm tides and also by extreme weather events. Sea level rises are expected due to the thermal expansion of oceans and the melting of mid-low and high latitude glaciers. An increase in temperature in the Antarctic region could initially lead to an increased accumulation of ice through snowfall, but this will be increasingly offset by increased meltwater, contributing to rises to sea level beyond the twenty-first century. Further research is needed to verify the impact of melting ice sheets on sea level rise.
- Significant uncertainties remain in relation to the estimation of future climate. These can be reduced by (1) improving the atmospheric and oceanic forcings input to future transient experiments, (2) improving the ability of GCMs to simulate ENSO behaviour under present and enhanced greenhouse conditions, and (3) improving the high resolution modelling of the region to better incorporate the effects of topography and air-sea interaction processes. Some of the improvements will be included in the IPCC AR5 simulations. Dynamical and statistical downscaling may also help.
- Climate impacts and adaptation assessments should be improved by further development of versatile climate impacts and adaptation models and methodologies for a number of key sectors and activities. These models should be developed and tested against observations initially. They can then be used to assess the impacts of more reliable climate change projections with reduced uncertainty when they become available. However, incorporation of the terrestrial carbon cycle and land cover changes into the new generation of GCMs may increase the uncertainty and hence the range of projected changes in the climate.

# Contents

<b>1.</b>	<b>Introduction .....</b>	<b>13</b>
1.1	Observed Climate and Climate Drivers .....	16
1.1.1	Atmospheric circulation patterns .....	16
1.1.2	Monthly mean winds .....	20
1.1.3	Monsoon and the wet season .....	21
1.1.4	Cold wind surges.....	24
1.1.5	Intra-seasonal Oscillation.....	25
1.1.6	El Niño-Southern Oscillation (ENSO).....	26
1.1.7	Pacific Decadal Oscillation (PDO).....	27
1.1.8	Tropical cyclones .....	28
1.1.9	Sea level rise .....	30
<b>2.</b>	<b>Observed surface temperature, net radiation, humidity and cloudy days ...</b>	<b>33</b>
2.1	Monthly net radiation, air temperature, relative humidity and number of cloudy days over the region .....	33
2.2	Regional Sea Surface Temperatures: Mean, Trends and Variability.....	34
2.3	Maximum, minimum and mean temperatures: Trends and variability at Thursday Island and Daru .....	37
2.4	Apparent temperature.....	38
<b>3.</b>	<b>Method for generating future climates .....</b>	<b>41</b>
3.1	Uncertainties associated with future projections. ....	41
<b>4.</b>	<b>Climate change projections .....</b>	<b>44</b>
4.1	Projected changes in solar radiation and temperature.....	44
4.2	Projected changes in rainfall, relative humidity and wind speed.....	46
4.3	Projected changes in potential evaporation .....	48
4.4	Projected changes in apparent temperature .....	48
<b>5.</b>	<b>Conclusions .....</b>	<b>50</b>
5.1	Observed and projected climates in the Torres Strait region .....	50
5.2	Potential climate change impacts in the Torres Strait region .....	51
5.3	Conclusions and recommendations .....	52
<b>6.</b>	<b>Knowledge gaps .....</b>	<b>54</b>
<b>7.</b>	<b>References .....</b>	<b>56</b>

## Table of Figures

<b>Figure 1.</b> The Torres Strait region. The yellow line delimits the Torres Strait Protected Zone established under the Torres Strait Treaty. The pink line delimits the inner islands. (Source: National Oceans Office). .....	13
<b>Figure 2.</b> Typical winds and synoptic features in January (a, left) and July (b, right). Source: Manins et al., 2001. ....	17
<b>Figure 3:</b> The domain used to calculate area-average rainfall is shown by a rectangle. Land-only areas have been used to calculate average rainfall. Colours represent rainfall amounts (mm/day). .....	18
<b>Figure 4:</b> Average composite differences in 925 hPa winds and OLR values. The left figure shows the pattern for 1951-1976 and the right figure the pattern for 1977-2007 .....	18
<b>Figure 5:</b> Average composite difference in rainfall and pressure. Pressure values are shown by contour lines and colours depict rainfall anomalies. The left figure is for the period 1952-1976 and the right figure is for the period 1977-2007. ....	19
<b>Figure 6.</b> Monthly wind directions (arrows) and speed (m/sec) in colours over the Torres Strait region from October to April. Source: NCEP Reanalysis. ....	20
<b>Figure 7.</b> Monthly wind directions (arrows) and speed (m/sec) in colours over the Torres Strait region from May to September. Source: NCEP Reanalysis. ....	21
<b>Figure 8.</b> Annual rainfall at Daru and Thursday Island. Note the coherent variability at these stations on the inter-annual time scale. ....	22
<b>Figure 9.</b> Annual rainfall variations in the southern part of the Torres Strait (from three stations).....	22
<b>Figure 10.</b> October to April rainfall at Thursday-Horn Islands. ....	23
<b>Figure 11.</b> October to April rainfall variation at Daru. ....	23
<b>Figure 12.</b> May to September rainfall variation at Thursday-Horn Islands. ....	24
<b>Figure 13.</b> May to September rainfall variation at Daru. ....	24
<b>Figure 14.</b> Mean daily rainfall variations at Thursday Island. ....	25
<b>Figure 15.</b> Mean daily rainfall variations at Daru. ....	26
<b>Figure 16.</b> Relationship between October to April rainfall at Thursday Island and the SOI (October to April). ....	27
<b>Figure 17.</b> Year to year variability in Thursday Island wet season (October to April) rainfall and the SOI (October to April). ....	27
<b>Figure 18.</b> Tropical storms and cyclones that fall between Category 1 and 5 in the vicinity of the Torres Strait region. Only tracks from 1970 and 2008 are plotted as records prior to this are not reliable. Source: US National Climatic Data Center, Ashville. ....	29
<b>Figure 19.</b> Tropical cyclone tracks of Category 1 to 5 that occurred over northeast Queensland and the vicinity of the Torres Strait region. Source: US National Climatic Data Center, Ashville. ....	29

<b>Figure 20.</b> Mean sea level measured at Booby Island. Source: Australian Bureau of Meteorology. ....	30
<b>Figure 21.</b> Mean Sea level changes in the Torres Strait region. Source: Colorado State University. ....	31
<b>Figure 22.</b> Projected mean sea level rise (m) for the 21 <sup>st</sup> century. Source: IPCC 2007. ....	32
<b>Figure 23.</b> (a) Mean monthly values of net radiation, (b) surface temperature at 2 metres, (c) relative humidity at 2 metres and (d) cloud cover in the Torres Strait region. Net radiation units (Watts per square metre), surface temperature (°C) and, relative humidity (%) and cloud cover (%). The region is defined here as the grid between 9-11°S and 141-145°E. Source: NCEP reanalysis. ....	33
<b>Figure 24.</b> Annual sea surface temperature in the Torres Strait region. Source: Australian Bureau of Meteorology.....	34
<b>Figure 25.</b> Seasonal sea surface temperatures in the Torres Strait region. Source: Australian Bureau of Meteorology. ....	35
<b>Figure 26.</b> Trends in sea surface temperature in the Torres Strait region. Trends are calculated from 1950 to present and shown as °C per decade. Source: Australian Bureau of Meteorology.....	35
<b>Figure 27.</b> Sea surface temperature anomalies (relative to the 1961-1990 mean) for both the northern wet (October-April) and dry (May – September) seasons. Vertical red bars indicate actual anomalies and the black line shows decadal-scale variations and trends. (Source: Australian Bureau of Meteorology). ....	36
<b>Figure 28.</b> Mean monthly temperatures at Daru and Thursday Island. ....	37
<b>Figure 29.</b> Trends and variability in annual (red lines), wet (blue lines) and dry (green lines) seasons temperature at Thursday Island and Daru. TIMO: Thursday Island Met. Office, TITS: Thursday Island Township and HI: Horn Island. Source: Australian Bureau of Meteorology and National Weather Service, Papua New Guinea.....	38
<b>Figure 30.</b> Monthly apparent temperatures for the Torres Strait region. The region is defined here as the grid between 9-11°S and 141-145°E. Source: NCEP reanalysis. ....	39
<b>Figure 31.</b> Year to year variability in annual, wet and dry season apparent temperatures in the Torres Strait region. ....	40
<b>Figure 32.</b> Atmospheric concentrations and emissions of carbon dioxide, methane and nitrous oxide for six SRES scenarios. Source: Nakićenović and Swart (2000).....	42
<b>Figure 33.</b> Changes, relative to the average for the period 1980-2000 in global average surface temperature for the 21 <sup>st</sup> Century for the A1B, A1FI, A1T, A2, B1 and B2 SRES emissions scenarios. The dark shaded areas represent uncertainties in changes based on the consideration of the response of 19 climate models to the emissions scenarios. The light shaded areas represent uncertainties in changes based on the consideration of the response of the models to the emissions scenarios and uncertainty in carbon cycle feedbacks in the climate system. The coloured lines indicate changes based on the mean average response of the models and mid-range assumptions about carbon cycle feedbacks. The black line indicates changes recorded during the 20 <sup>th</sup> Century. Source: Meehl et al. (2007b).....	42

## Table of Tables

Table 1. Projected changes in solar radiation (%) for A2 and (b) A1FI emission scenarios for 2030, 2050 and 2070. Changes are based on simulations from 22 models. ....	44
Table 2. Changes in maximum, minimum and mean temperatures for A2 (a to c) and A1FI (d to f) emission scenarios for 2030, 2050 and 2070. Results from 8 models have been used to construct projections for maximum and minimum temperatures and from 24 models for mean temperature. ....	45
Table 3. Projected changes in rainfall (a and b), relative humidity (c and d) and wind speed (e and f) for SRES A2 and A1FI emission scenarios for 2030, 2050 and 2070. Changes in all three variables are shown as percentages. Simulations of 24 models were used in projecting rainfall, 13 models for relative humidity and 19 models for wind speed. ....	47
Table 4. Projected changes (%) in potential evaporation for (a) A2 and (b) A1FI emission scenarios for 2030, 2050 and 2070 from 13 models. ....	48
Table 5. Projected increases in apparent temperatures for SRES (a) A2 and (b) A1FI emission scenarios for 2030, 2050 and 2070. Changes are shown in percentage. ....	49

# 1. INTRODUCTION

The Torres Strait Island region extends from the Cape York Peninsula to within 5 km of the Papua New Guinea (PNG) coastline (Figure 1). The outer islands consist of the western islands (Badu, Moa, Mabuiag), the north-western islands (Boigu, Dauan, Saibai), the eastern islands (Ugar, Erub, Mer) and the central islands (Masig, Poruma, Warraber, Iama). Thursday and Horn islands are located in the southern part of the region. Recent estimates show the population of the Torres Strait at about 6500, with 3500 living on either the administrative centre of Thursday Island or on nearby islands, and the remainder living on 13 of the outer islands (Briggs, 2010).

The Torres Strait region has diverse marine and fishery resources which are bases for the region's future economic development (TSRA, 2010). Some species are over-fished while there is uncertainty about the status of others. Key community-driven policy initiatives aiming to achieve sustainable economic and cultural development include the Torres Strait Regional Authority (TSRA) Land and Sea Management Strategy, the Torres Strait and Northern Peninsula Area Regional Plan, and the Torres Strait Development Plan. The indigenous people of the Torres Strait have a distinct culture which is slightly different to other indigenous Australians. Archaeological, linguistic and folk history evidence suggests that the core of Island culture is linked to Australia and other Pacific islands. People from these islands were traditionally agriculturalists although they supplemented their food supplies through hunting and gathering. The economy of the region is to mainly rely on fishing, pearl industry, sponge farming and tourism (TSRA, 2010).

Sponges are a key representative group throughout the coral reefs of the Torres Strait region. They play important functional roles in coral reef ecosystems and other several species and also show commercial potential for use as biomaterials (Whalan, 2009). This is a growing industry in terms of economy and employment.



**Figure 1.** The Torres Strait region. The yellow line delimits the Torres Strait Protected Zone established under the Torres Strait Treaty. The pink line delimits the inner islands. (Source: National Oceans Office).

Due to its location, the Torres Strait Region experiences a wet-dry climate. The mean annual temperature is around 27°C with a relatively small range from 25 °C to 28 °C. Most of the rainfall is received during the Australian monsoon season with little falling during the dry season, when the south-east trades dominate. The climate varies on time scales from weekly to several decades. It is influenced by the Australian monsoon, cold wind surges from south-east Asia, intra-seasonal variations or climate variations within the season, inter-annual variations associated with the El Niño-Southern Oscillation(ENSO) phenomenon, tropical cyclones and variations on multi-decadal time scale associated with Pacific Ocean Sea Surface Temperatures (SSTs).

There are no Australian Bureau of Meteorology high-quality data stations in the region. However, weather stations at Thursday Island and Horn Island (operated by the Australian Bureau of Meteorology) and a station on the southern part of Papua New Guinea (Daru) provide data that have not been quality controlled. These data, if used with care, provide general information on the present climate variability in the region. Variability from daily to inter-annual time scales and sometimes decadal-timescale can also be detected using data from these stations. Data from the Australian mainland (Cape York Peninsula and the Wet Tropics) have also been used to derive some of the conclusions in this report. In addition, long-term climatological information is also derived from large-scale data sets, such as the National Center for Environmental Prediction (NCEP) re-analysis dataset which covers ocean and land areas at coarse resolution (e.g. in the order of 250 km). Long-term climatological averages of surface winds, solar radiation absorbed at the surface, surface temperature, sea surface temperature and rainfall are calculated and then their spatial and temporal characteristics are discussed. Monthly values of these variables are also used to calculate apparent temperature in the region.



**Photo 1.** Iama Island. (Source TSRA).

Climate change projections are provided based on simulations from 24 GCMs used for the Intergovernmental Panel on Climate Change (IPCC) Fourth Assessment Report (IPCC, 2007). We provide climate change projections based on mid and high emission scenarios. Projected changes in climate variables are expressed in terms of 50<sup>th</sup>, 10<sup>th</sup> and 90<sup>th</sup> percentiles. The 50<sup>th</sup> percentile represents the median or mid value, while 10<sup>th</sup> and 90<sup>th</sup> percentiles represent lower and upper ranges of projections.

The specific objectives of this report are to:

- (a) Provide a discussion on observed climate and climate drivers of the region and trends and variations in observed climate variables, such as, temperature rainfall, solar radiation, cloudy days, etc.*
- (b) Provide a description of the methodology and its related uncertainties used to generate climate change projections.*
- (c) Provide climate change projections for a number of simulated variables*
- (d) Indicate the uncertainties in the climate change projections.*



**Photo 2.** Thursday Island. Looking towards the south from Green Hill. (Source R. Suppiah).



**Photo 3.** Saibai Island. (Source TSRA).



**Photo 4.** Warraber Island. (Source TSRA).

## **1.1 Observed Climate and Climate Drivers**

### **1.1.1 Atmospheric circulation patterns**

During summer, the Australian monsoon brings humid and rainy conditions to northern Australia. On average, the arrival ('onset') of the monsoon occurs between late December and early January (long-term average December 28) (McBride, 1987; Suppiah, 1992). Strong westerly winds and heavy rainfall are associated with the onset. The monsoon trough (red dashed line in Figure 2a), a low pressure area between the equatorial north-west winds and the south-east trades, tends to dominate the weather during this season (Figure 2a). A fully developed monsoon circulation system is comprised of at least three distinct weather patterns: *the active, moderate and break phases* of the monsoon. Their occurrence is associated with variations in the

strength of the entire monsoon system within seasons and from year to year. The active phase is more energetic than the moderate phase, with stronger westerlies, an intense tropical monsoon trough and enhanced rainfall. Intense depressions and tropical cyclones often form during the active phase along the monsoon trough. The break, or dormant phase, is associated with weak westerlies and little or no rainfall, while the moderate phase has average monsoon conditions, between active and break phases. The monsoon is one of the dominant climate drivers that affects the climate and climate variability of the Torres Strait region.

Seasonal westerly winds dominate the climate as the summer approaches (Figure 2a), while south-east trades dominate the winter/dry season (Figure 2b). Winds from the northern hemisphere reach the region after collecting moisture from the Indonesian region and give enhanced rainfall from December to March. This type of synoptic situation is clearly evident during heavy rainfall events in tropical rainforest, Cape York and Torres Strait regions (Manins *et al.*, 2001).

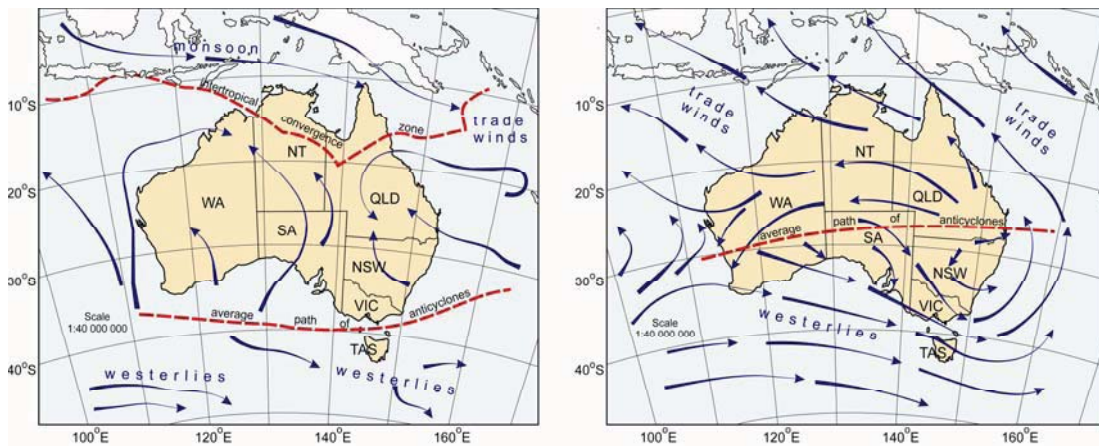


**Figure 2.** Typical winds and synoptic features in January (a, left) and July (b, right). Source: Manins *et al.*, 2001.

Examples of synoptic situations and their associated patterns of sea level pressure, out-going long-wave radiation (OLR, a measure of large-scale convection derived from satellites observations) and rainfall are shown here as differences between the composites based on heavy and low rainfall days. Heavy rainfall days are defined as days that received daily rainfall above the long-term average of the 90<sup>th</sup> percentile. Low rainfall days are defined as days that received rainfall below the long-term average of the 10<sup>th</sup> percentile. Here, the difference between the composite of 90<sup>th</sup> percentile events and 10<sup>th</sup> percentile events are shown in Figures 4 and 5 as the regions of important can be seen clearly. During this time of the year (wet season), access to the area is via air and sea.

Figure 4 shows average composite differences in OLR and winds for periods between heavy and low rainfall days for two periods: 1950-1976 and 1977-2007. During heavy rainfall events, an area of active convection is noticed over a broad region centred on far northeast Queensland. This active convection area, which covers the Indonesia-north Australia region, is shown by strong negative OLR values. Stronger north-easterlies over south-east Asia, stronger westerlies over the Indonesia-north Australia region and a distinct cyclonic (where horizontal flow is in a clockwise direction) type circulation over the Coral Sea are also identified. The evolution of extreme events in winds and OLR values suggests a gradual strengthening of winds over south-east Asia

and the Indonesian-north Australian region. Winds associated with the large-scale convective system tend to become weaker after peak events and dissipate after about two weeks.

Rainfall and mean sea level pressure average composite differences show low pressure and heavy rainfall over far north Queensland. Heavy rainfall and an active convective system are indicated by strong negative OLR values. Wind and pressure patterns suggest these events are part of a large-scale circulation pattern.

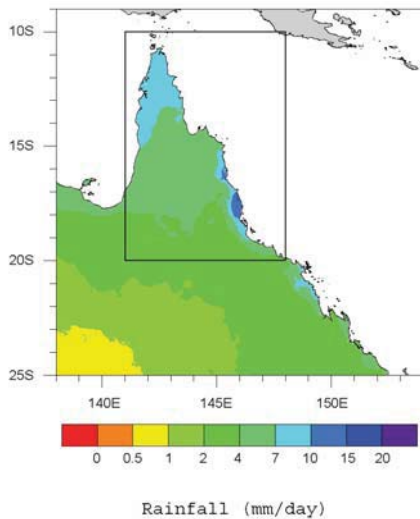


**Figure 3:** The domain used to calculate area-average rainfall is shown by a rectangle. Land-only areas have been used to calculate average rainfall. Colours represent rainfall amounts (mm/day).

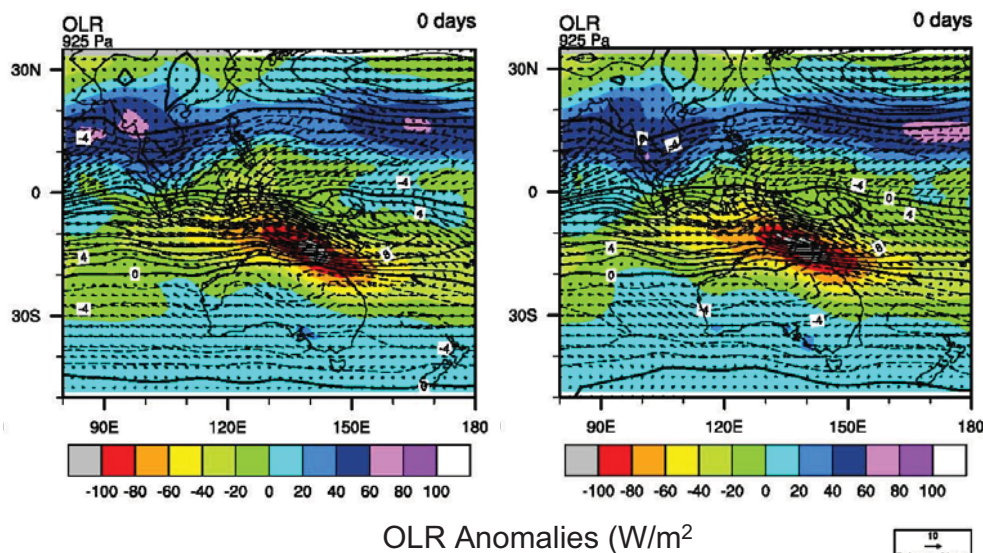
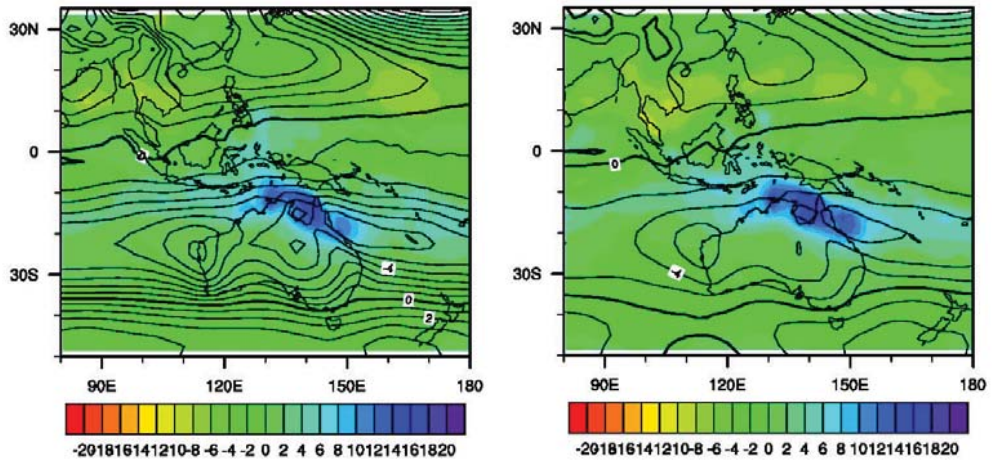


**Figure 4:** Average composite differences in 925 hPa winds and OLR values. The left figure shows the pattern for 1951-1976 and the right figure the pattern for 1977-2007.



Rainfall anomalies (mm/day)

**Figure 5:** Average composite difference in rainfall and pressure. Pressure values are shown by contour lines and colours depict rainfall anomalies. The left figure is for the period 1952-1976 and the right figure is for the period 1977-2007.



**Photo 5:** Inundation in the Saibai Island. (Source TSRA).

Extreme rainfall events associated with active monsoon activity cause extensive damage to properties, human life and day-to-day activities in the region. Large swells and build-up of water during the monsoon season associated with extreme winds and rainfall change the topographical/geomorphological characteristics of the coast (Parnell and Smithers, 2010). Therefore, any strengthening of the monsoon over time could have significant effects on the environment of the islands.

### 1.1.2 Monthly mean winds

Monthly mean wind directions and speed from October to April in the Torres Strait region are shown in Figure 6. Mean wind directions and speed are from the NCEP reanalysis dataset which has a coarse resolution of 250 km. However, it is possible to derive some conclusions about the circulation patterns in the region. South-easterlies dominate October and November, before the onset of the Australian monsoon and in March and April after the monsoon season. The period from December to February is dominated by westerly and north-westerly winds. In particular, January and February are the months with strong north-west winds. Average monthly wind speeds reach 7-8 m/sec in October and 3-4 m/sec during the monsoon. Wind speed can be much higher during onset and active periods of the monsoon, sometimes as high as 10-15 m/sec (Suppiah and Wu, 1998).

South-easterlies dominate the circulation pattern between May and September as shown in Figure 7. Wind speeds are relatively stronger than wet season months. Monthly average wind speeds range between 7-10 m/sec in most areas.

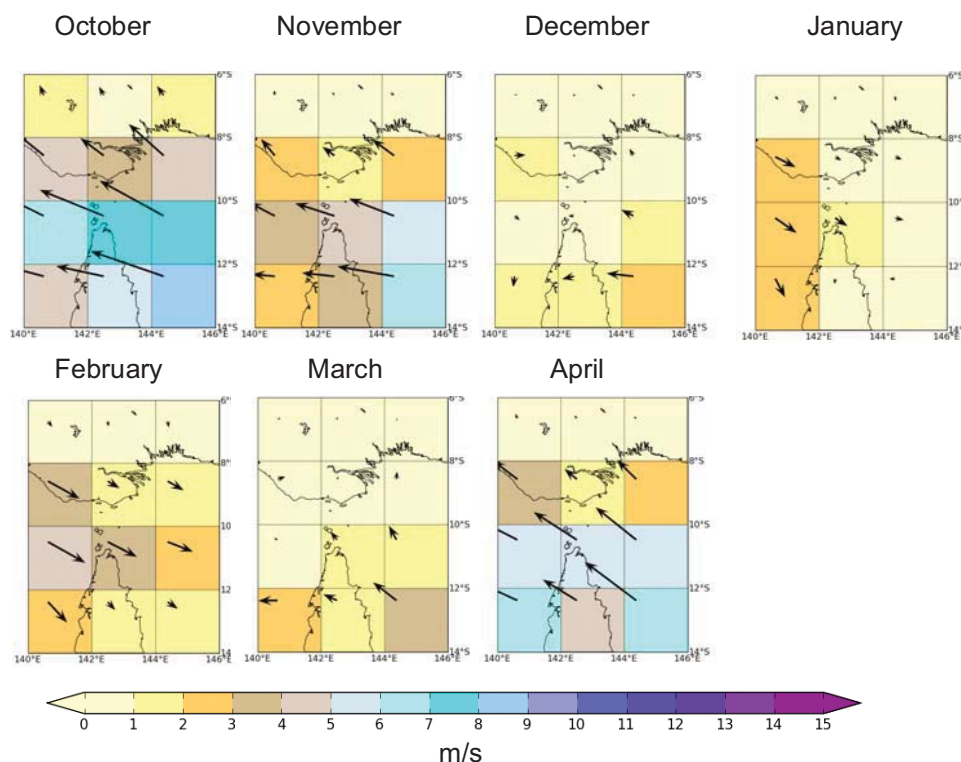


**Figure 6.** Monthly wind directions (arrows) and speed (m/sec) in colours over the Torres Strait region from October to April. Source: NCEP Reanalysis.

### 1.1.3 Monsoon and the wet season

There are two distinct climatic seasons in the Torres Strait region, the 'wet' and 'dry' seasons. The wet season (locally known as '*kuki*') typically occurs from December to April, while the dry season begins in May and ends in December (TSRA, 2010). Annual rainfall is about 1800 mm which occurs mainly during the summer months. The wet season with higher rainfall and humidity is primarily linked to the Australian summer monsoon. Data from three nearby meteorological stations were used to construct a long time-series for analysis of decadal-scale variations. The stations used were Thursday Island Meteorological Office (TIMO), Thursday Island Township and Horn Island all of which are Australian Bureau of Meteorology stations. These represent the southern part of the region. We also used data for Daru, located in the southern part of Papua New Guinea to represent the northern part of the region. Annual rainfall variations from Thursday Island and Daru are shown in Figure 8 indicating that these regions are strongly correlated on year-to-year time scales. The correlation coefficient between these time series is 0.45 for the same period, which is statistically significant at the 95% confidence level. Thursday Island receives about 1750 mm and Daru receives about 1980 mm. However, there are significant seasonal differences between measures of dry season rainfall between these stations, which will be discussed later.

Reconstructed annual rainfall for the southern part of the region (Figure 9) shows strong variations on inter-annual and inter-decadal time scales. The 1960s and 1990s were dry and the 1970s and recent years were relatively wet. This is also true for the northern part as shown by Daru rainfall.

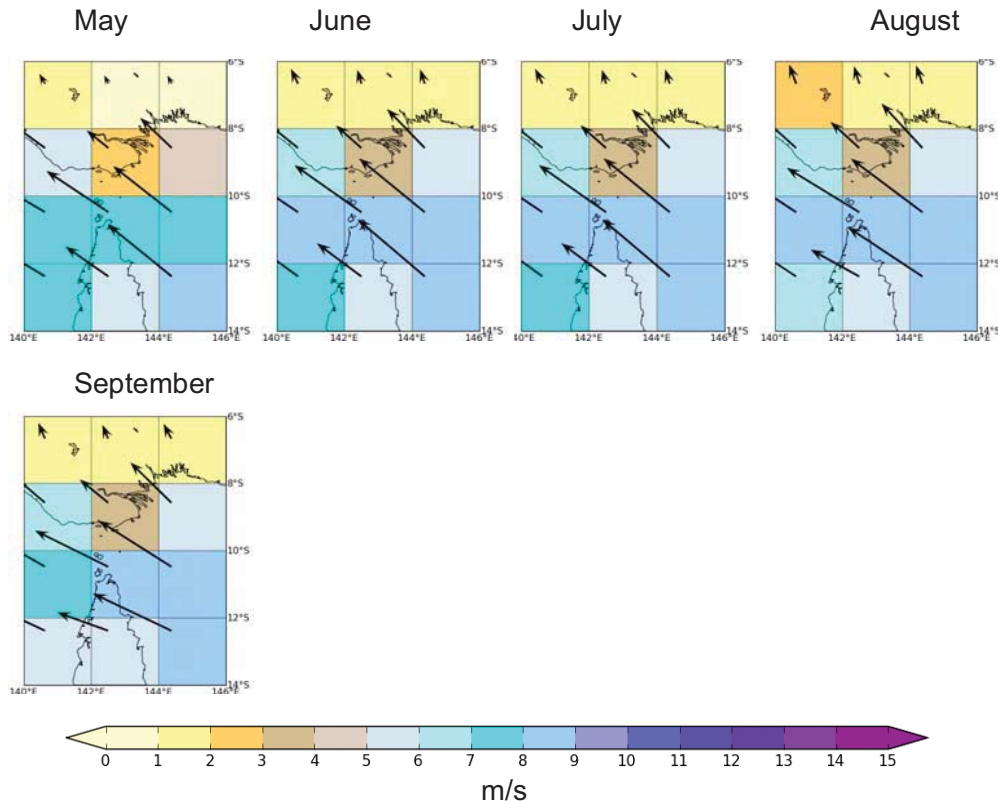


**Figure 7.** Monthly wind directions (arrows) and speed (m/sec) in colours over the Torres Strait region from May to September. Source: NCEP Reanalysis.

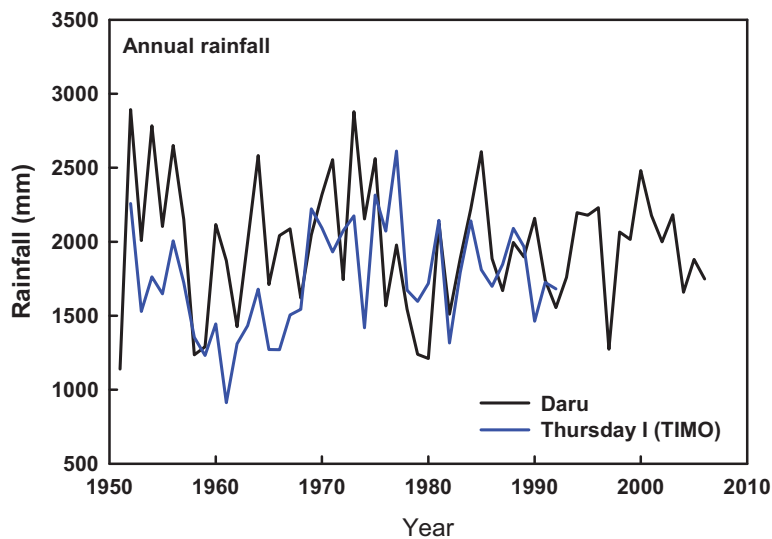


**Figure 8.** Annual rainfall at Daru and Thursday Island. Note the coherent variability at these stations on the inter-annual time scale.

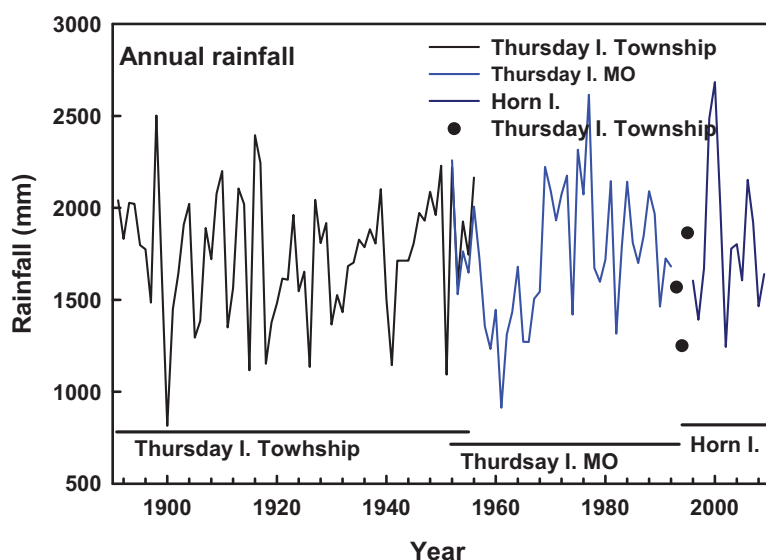


**Figure 9.** Annual rainfall variations in the southern part of the Torres Strait (from three stations).

October to April rainfall in the southern part of the Torres Strait region primarily dominates inter-annual and inter-decadal variations, as little rainfall is received during the dry season. The average wet season rainfall is about 1640 mm. Figure 10 shows extremely wet and dry periods during the past century. In particular, the 1960s and the 1990s were dry and 1970s and 2000s were wet periods. Rainfall variations before 1950 show strong inter-annual variations. Although the rainfall time series was constructed from three nearby stations, it is unlikely that inter-annual and inter-decadal variations are affected by such a construction. Wet season rainfall in Daru is slightly less than Thursday Island due to the location of the station. Daru receives about 1500 mm during the wet season and shows strong inter-annual and inter-decadal variations compared to Thursday Island (Figure 11).

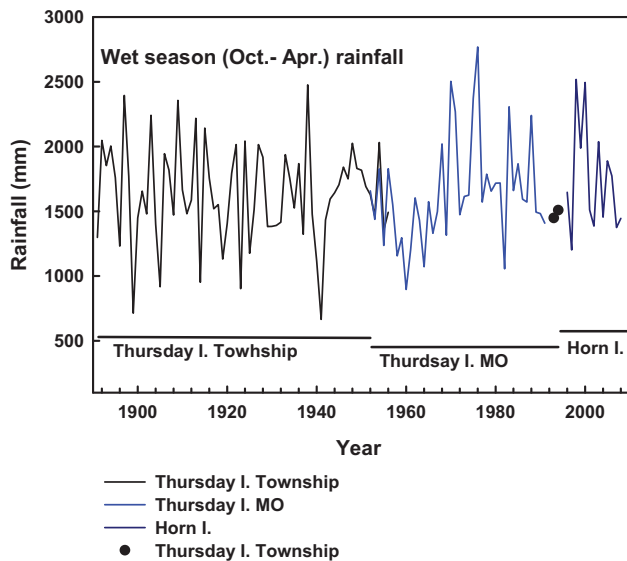


**Figure 10.** October to April rainfall at Thursday-Horn Islands.

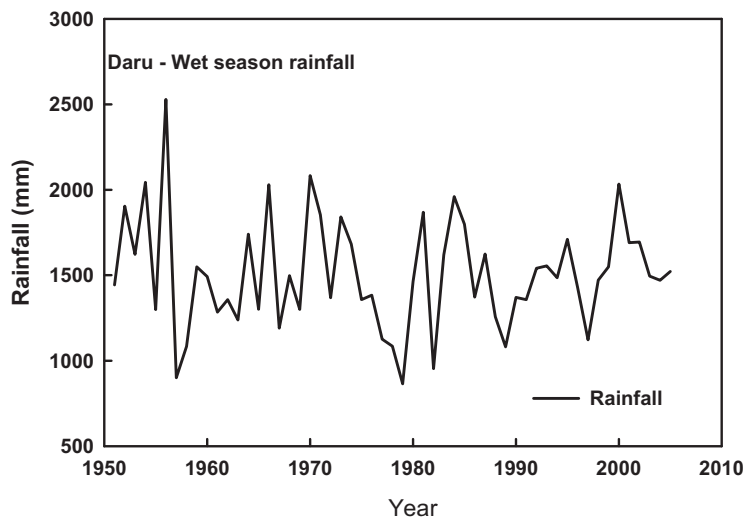


**Figure 11.** October to April rainfall variation at Daru.

The dry season is characterised by sunny days with very little or no rain. During this season, *trade winds* dominate the weather and climate of the region and the season is locally known as ‘*Sager*’. South-easterly trade winds bring moisture to most of the north-east coast of Australia, but little rain to the region, particularly in the southern part. However, the northern part of the region does receive some rainfall from south-east trades as shown by the Daru data. The effect of south-easterly winds has greatest effect between May to September. Trade winds not only give little rainfall to the southern part of the region, but also affect waves and tides in this region. During the dry season, Thursday Island receives about 90 mm, while Daru receives about 480 mm. Although mean rainfall is low during this season, there were some years with extreme rainfall events in this region shown both at Thursday Island and Daru. These variations are shown in Figures 12 and 13.

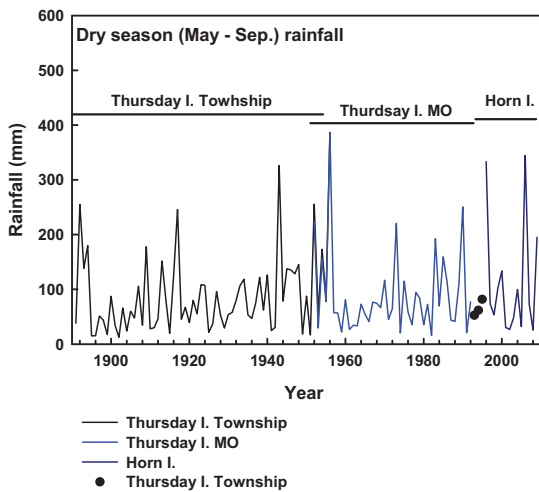


**Figure 12.** May to September rainfall variation at Thursday-Horn Islands.

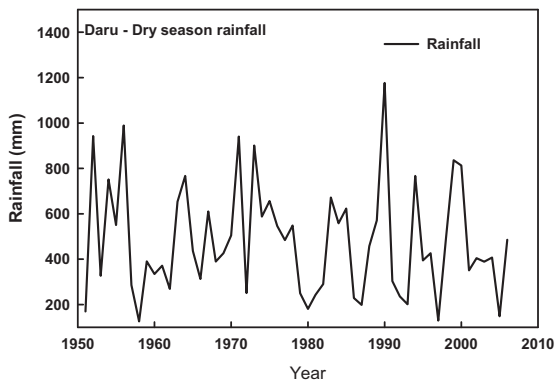


**Figure 13.** May to September rainfall variation at Daru.

The transition from the dry season to wet season is characterised by weak northerly winds which blow intermittently between October and December. This season is known locally as 'Naigai' and characterised by a sustained increase in temperature and humidity. Southerly winds which blow randomly throughout the year are called locally 'Zay'.

#### 1.1.4 Cold wind surges

Cold wind surges, which mainly develop over East Asia, propagate towards northern Australia after crossing the South China Sea. Strong winds and heavy rainfall are associated with these cold surges, particularly during the Australian monsoon season. The frequency of strong wind events is usually high before the onset and active phase of the monsoon. A number of studies have reported the influence of cold surges from south-east Asia on the weather and climate of northern Australia, particularly during the summer monsoon season (e.g. Webster, 1981; Love, 1985; Suppiah and Wu, 1998). Strengthening of winds over south-east Asia before the Australian monsoon was reported by Davidson (1984). Keenan and Brody (1988) showed that cold surges act as triggering mechanism for Australian monsoon activity. Cold wind surges during the

Australian monsoon approach the Torres Strait region from the northern hemisphere through south-east Asia. This is clearly seen in Figure 4 which is based on composite extreme rain events. Floods and wind damage are associated with cold surges and can increase the risk of diseases from flooded rubbish tips, affecting sewerage systems and changing mosquito habitats. Moreover, erosion of roads, airstrips and buildings and graveyards near the shoreline can be affected by intense storm tides.

### 1.1.5 Intra-seasonal Oscillation

Rainfall variation within seasons is influenced by the tropical intraseasonal oscillation (ISO), which has a period ranging between 30 and 50 days. The frequency and magnitude of this oscillation are both linked to the El Niño-Southern Oscillation (ENSO) phenomenon. During the monsoon season, there are periods of heavy and persistent rain and also periods with little or no rain, the former called the “active monsoon period” and the latter called the “break monsoon period”. Such periodic variations are not random events within the monsoon season, and are associated with global-scale variations on similar time scale. The intra-seasonal Oscillation (ISO) was first described by Madden and Julian (1971) in the early 1970s. Therefore, this oscillation is also referred to as the Madden-Julian Oscillation.

The ISO is apparent in winds, cloud and rainfall variations in the tropics. In the Australian tropics, the existence of ISO has been reported in Outgoing Long-wave Radiation (OLR), winds and rainfall (Hendon and Liebmann, 1990; Suppiah, 1993; Wheeler and McBride, 2005). OLR provides a measure of convection/rainfall from satellite observations. Daily rainfall variations at Thursday Island (Figure 14) are consistent with variations due to ISO and coincide with the wet season. The first peak appears in association with the onset of the monsoon and subsequent peaks show active periods of the monsoon. Daily rainfall in the northern part of the region also shows variability on this time scale with the greatest variability at the end of the wet season, as shown by Daru rainfall (Figure 15). Such a difference in variability can arise from the effects of other atmospheric mechanisms at both shorter and longer periods.

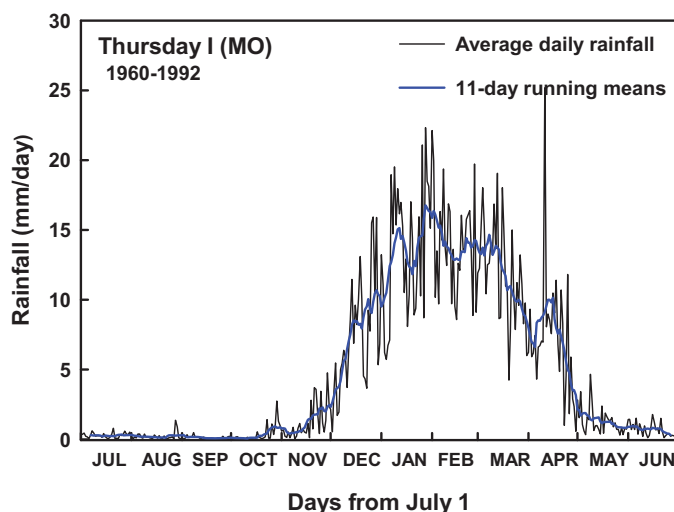


**Figure 14.** Mean daily rainfall variations at Thursday Island.

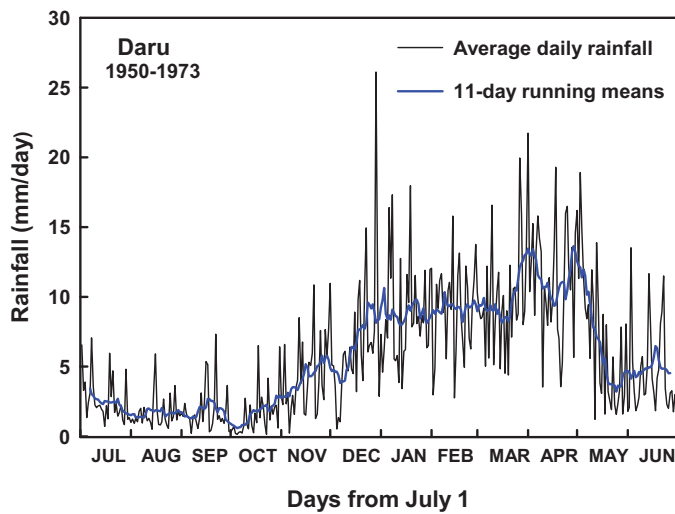


**Figure 15.** Mean daily rainfall variations at Daru.

### 1.1.6 El Niño-Southern Oscillation (ENSO)

El Niño-Southern Oscillation (ENSO) events affect the climate of the region and can be monitored using the Southern Oscillation Index (SOI), a measure of the pressure difference between Darwin and Tahiti. El Niño events are associated with warmer sea surface temperatures in the central and eastern Pacific Ocean and weak trade winds and westerly wind bursts along the Equator. El Niño events are also associated with higher than normal pressure in the Indonesia-north Australia region and lower than normal pressure in the Central Pacific. The term La Niña refers to a phase opposite to an El Niño phase. The La Niña events are associated with positive SOI values, while El Niño events are associated with negative SOI values. El Niño and the Southern Oscillation together comprise a complex system of climate variability presently known as the El Niño-Southern Oscillation (ENSO) phenomenon.

ENSO strongly influences the Torres Strait region and Australian regions on year-to-year time scales. Generally, it is the largest source of year-to-year variability affecting the climate of the region, as well as other parts of the tropics. Generally, La Niña years are associated with above-average rainfall and El Niño years are linked to below-average rainfall (e.g. McBride and Nicholls, 1983; Suppiah, 1992). A strong positive relationship between wet season rainfall and the SOI in Figure 16 indicates the strong influence of ENSO in rainfall in the region (the correlation coefficient of 0.41 is significant at the 95% confidence level). Most of the anomalous wet years in the region are linked to positive SOI values, and dry years coincide with negative SOI values, although there are a few exceptional years as depicted in Figure 17. ENSO not only influences rainfall but also influences the formation of tropical cyclones over the Australian region. Tropical cyclones tend to form closer to the east coast of Australia during La Niña years, while they form away from the continent during El Niño years (Hastings, 1990). Moreover, Smith et al. (2008) suggested that the onset of the wet season tends to occur earlier than usual during La Niña years and later in El Niño years.

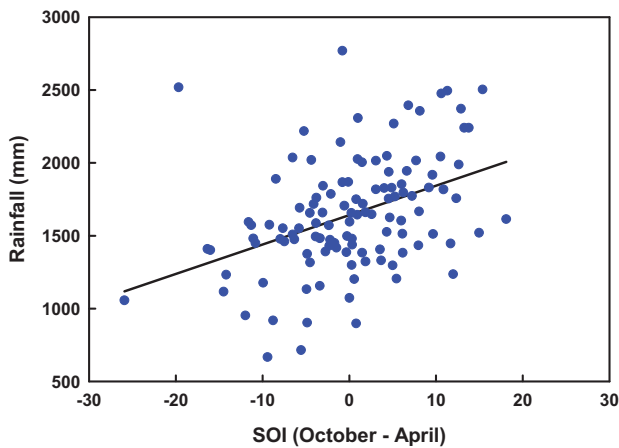


**Figure 16.** Relationship between October to April rainfall at Thursday Island and the SOI (October to April).

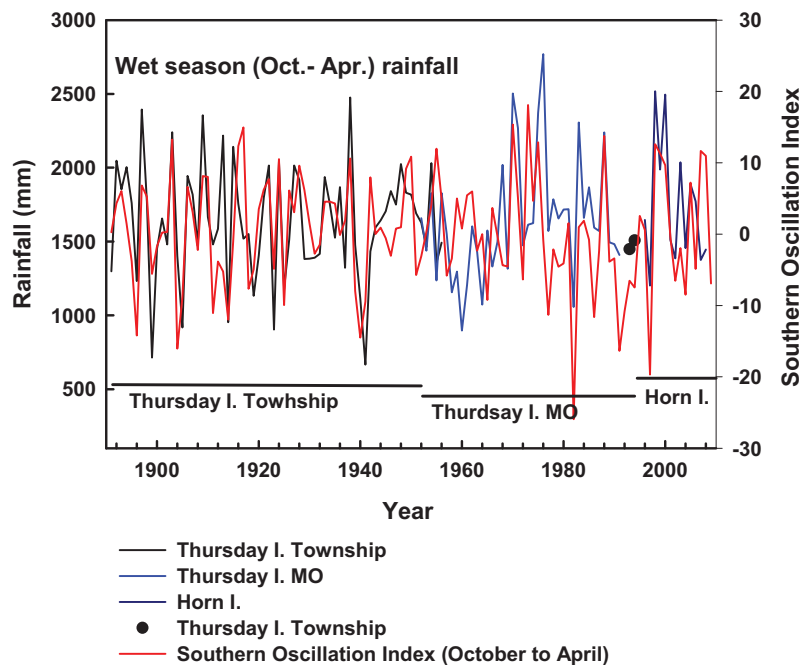


**Figure 17.** Year to year variability in Thursday Island wet season (October to April) rainfall and the SOI (October to April).

### 1.1.7 Pacific Decadal Oscillation (PDO)

Climate across the Pacific Ocean also shows evidence of strong variability on inter-decadal time scales. The Pacific Decadal Oscillation (PDO) has been linked to a long-lived El Niño-like pattern of Pacific climate variability (Mantua and Hare, 2002). However, there are conflicting views about the spatial and temporal characteristics of this oscillation (Folland *et al.*, 2002). This oscillation has two dominant periodicities, one from 15 to 25 years and the other from 50 to 70 years. Moreover, this oscillation is evident in sea surface temperature variations in the Pacific Ocean. Several studies reported two full independent cycles in the past century. Cool PDO regimes prevailed from 1890-1924 and again from 1947-1976, while warm PDO regimes prevailed from 1925-1946 and from 1977 to present. This low frequency (multi-decadal) oscillation,

which exists in sea surface temperature, is less confined to the equatorial belt in the central and eastern Pacific, but is more prominent over the extratropics, especially the North Pacific (Folland *et al.*, 2002; Power *et al.* 1999). The existence of the PDO in mean sea level pressure was also reported by Salinger *et al.* (2001).

The influence of the PDO on the climates of Australia, New Zealand and the Pacific has been reported in a number of studies (Power *et al.*, 1999; Salinger *et al.* 2001). The warm phase of November to April PDO temperature anomalies coincides with warm temperature anomalies over north-western Australia and also dry conditions in eastern Australia. In contrast, the cool PDO anomalies are associated with cool-wet conditions over north-western Australia. At present, the impact of the PDO on a small region, such as the Torres Strait region cannot be differentiated from the broader scale effects. Further research is needed to determine the influence on the climate of this region.

### 1.1.8 Tropical cyclones

Severe tropical cyclones are rare in the region. However, tropical cyclones crossing the Cape York Peninsula can pose a significant threat through stronger winds, waves and storm surges. Further details of the impacts of cyclones on the region can be found in Green *et al.* (2010). The formation of tropical cyclones in the Australian region is highly seasonal and is largely confined to the summer months, although tropical cyclones do form in late spring and early autumn. Monsoon depressions and tropical cyclones are responsible for large amounts of rainfall and damage during summer which form along the monsoon trough. Statistics on the formation of tropical cyclones near the region, except for the satellite era, are sparse. Figure 18 shows tracks of storms that include Category 1 to Category 5 cyclones between 1970 and 2008, a period with reliable data available from satellite pictures (National Climate Data Center, US, website). Most of the storms (Category 1 to Category 5) crossed over north-eastern Australia, but a few affected the Torres Strait region. In particular, very few severe storms affected the region between 1970 and 2008, although there is evidence of severe storm damage in the past (McBride and Keenan, 1982). Breakdowns of storm-tracks by category tracks are shown in Figure 19. This Figure shows the incidence of direct hits by severe tropical cyclones is low, but the indirect effect of cyclones that move towards the north-east coast of Australia can be significant through storm surges generated by these storms. Ocean inundation is a common hazard impacting many communities in the region associated with tropical cyclones and tropical depressions that form over Coral Sea.

There is a large uncertainty about changes to tropical cyclone behaviour due to enhanced greenhouse conditions. Solomon *et al.* (2007) reported that intensity of tropical cyclones will increase globally under enhanced greenhouse conditions, but a lack of regionally-specific information means it is difficult to state how any change in tropical cyclone activity may impact the Torres Strait Region (Green *et al.*, 2010). However, a recent review by Knutson *et al.* (2010) of tropical cyclone characteristics simulated by models suggests an increase in globally-averaged tropical cyclone intensity of 2-11% by 2100. This leads to an increase of the order of 20% in the precipitation rate within 100 km of the storm. These models also suggest a decrease in the frequency in the southern hemisphere with mixed changes over northern Australia. Further investigation is needed to establish the physical basis and statistical significance of these changes to understand the effects of tropical cyclones in the region under enhanced greenhouse conditions.



**Photo 6.** Saibai – Children playing in receding flood waters. (Source TSRA).

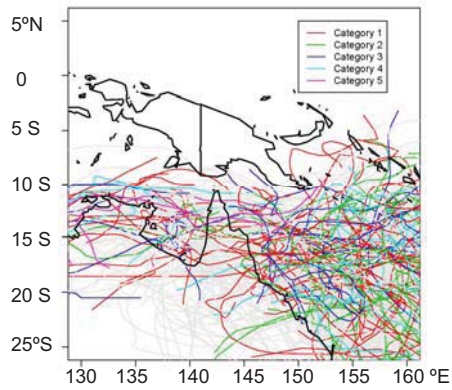


**Figure 18.** Tropical storms and cyclones that fall between Category 1 and 5 in the vicinity of the Torres Strait region. Only tracks from 1970 and 2008 are plotted as records prior to this are not reliable. Source: US National Climatic Data Center, Ashville.

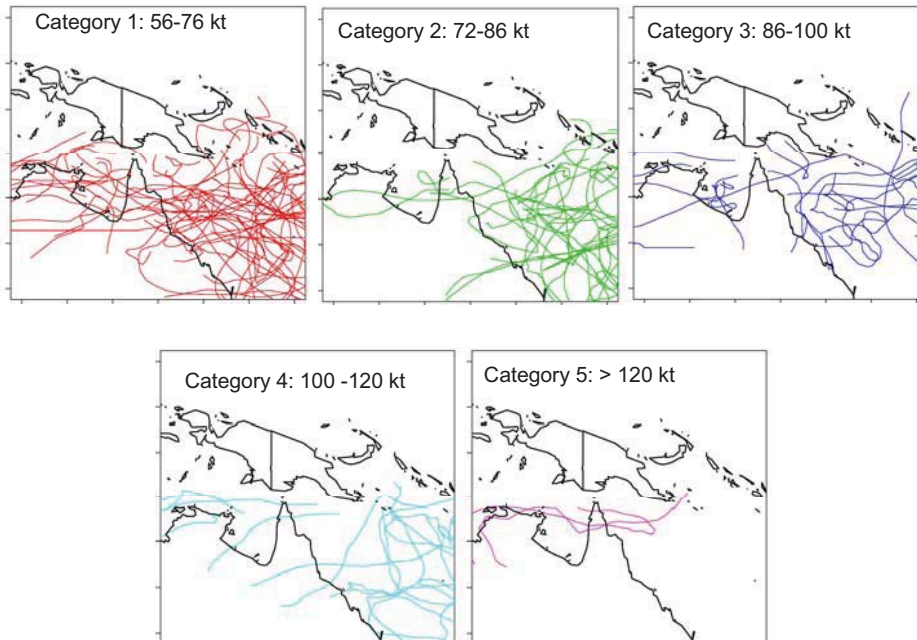


**Figure 19.** Tropical cyclone tracks of Category 1 to 5 that occurred over northeast Queensland and the vicinity of the Torres Strait region. Source: US National Climatic Data Center, Ashville.

### 1.1.9 Sea level rise

Sea level rise is one of the greatest threats to the Torres Strait region. Long-term mean sea level change and its variability is of considerable interest in the studies of global climate change, as this can be a threat to coastal regions and island nations. Long-term sea level variations are primarily determined with two different methods. One is estimated from tide gauge measurement by long-term averaging and the other is from satellite measurements. Reliable estimates of global mean sea level rise from satellite altimetry first became possible with the launch of the TOPEX/Poseidon radar altimeter satellite (T/P) in 1992. Regional and global estimates of mean sea level rise are given in Mitchum et al. (2010). Mean sea level of the region shows a strong annual cycle associated with summer monsoonal winds and winter south-easterlies. Figure 20 shows mean sea level measured from Booby Island. It is evident that sea level measurements show a strong seasonal cycle, indicating relatively higher sea levels during the Australian summer monsoon season and lower during the dry season. Short-term variability in sea level in the region is associated with storm surges, wind-driven circulation associated with surges from south-east Asia and tropical storms and cyclones in the Coral Sea area. Inter-annual variability in the sea level is strongly associated with ENSO variability. Sea level anomalies from a grid point in the Torres Strait region (10°S, 142°E) in Figure 21 show an increasing trend with strong short-term and inter-annual variability. Changes in mean sea level is 6 mm per year between 1993 and 2010 for the region, which is twice the global average sea level change (3 mm per year) given by Mitchum et al. (2010). Apart from a positive trend, this Figure also shows strong inter-annual variability associated with ENSO. Sea levels were lower during El Niño years and higher during La Niña years. The El Niño years, such as 1997-1998, 2002-2003 and 2006-2007 show negative anomalies of sea level.

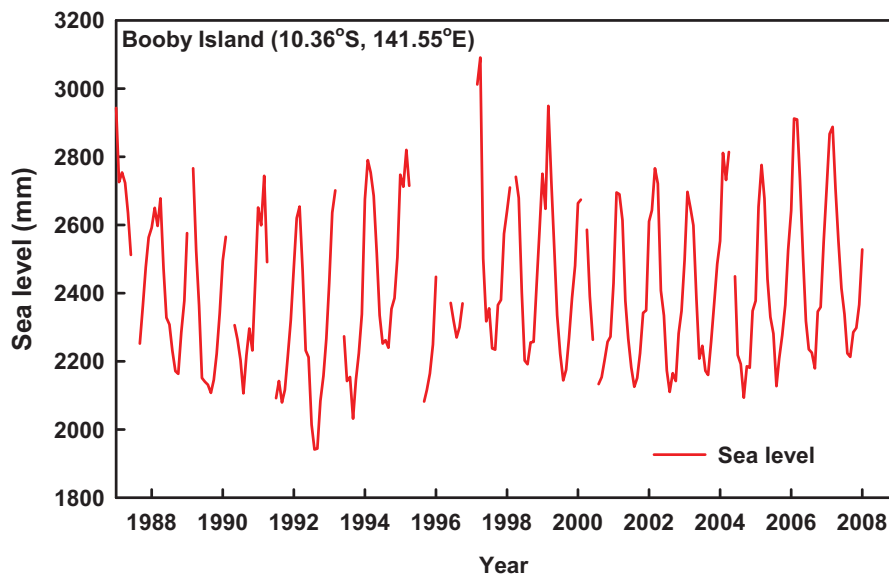


**Figure 20.** Mean sea level measured at Booby Island. Source: Australian Bureau of Meteorology.

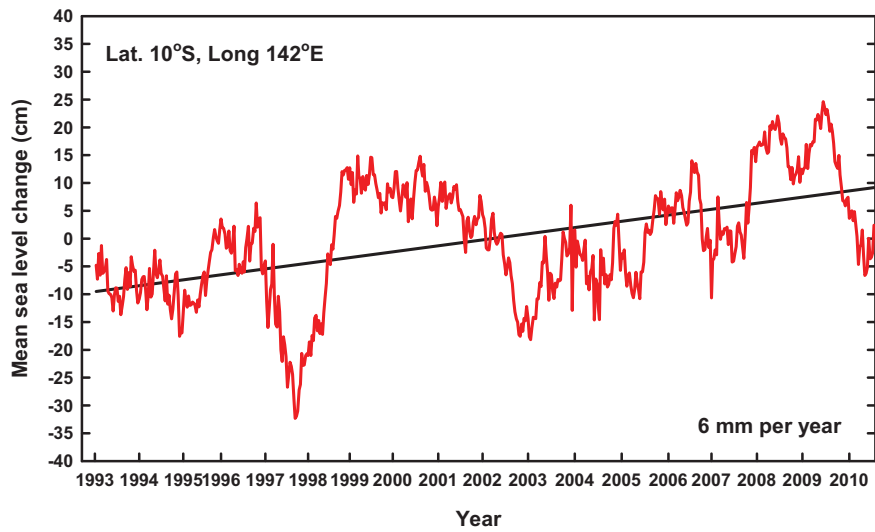


**Figure 21.** Mean Sea level changes in the Torres Strait region. Source: Colorado State University.



**Photo 7.** Saibai – community built seawall – January 2011 spring tide. (Source TSRA)

Sea level rise projected by IPCC (2007) is shown in Figure 22. Rises in sea level are expected due to thermal expansion of oceans and melting of mid-low and high latitude glaciers. Sliding ice sheets due to melting in Antarctica and Greenland can significantly contribute to further increases in sea level rise. However, extreme sea levels projected by IPCC with combination of these factors and others can not be ignored.

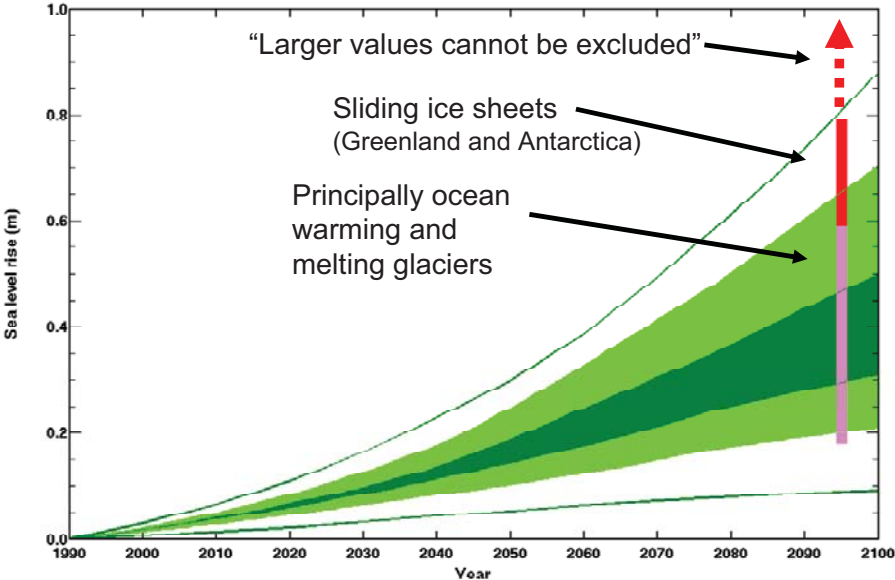


**Figure 22.** Projected mean sea level rise (m) for the 21<sup>st</sup> century. Source: IPCC 2007.



**Photo 8.** Protection against erosion in Thursday Island. (Source R. Suppiah).

## 2. OBSERVED SURFACE TEMPERATURE, NET RADIATION, HUMIDITY AND CLOUDY DAYS

### 2.1 Monthly net radiation, air temperature, relative humidity and number of cloudy days over the region

In this section, we provide long-term climatologies of net (downward minus upward) radiation, air temperature at 2 metres, relative humidity at 2 meters and cloudy days. Monthly mean net radiation averaged over the Torres Strait region is shown in Figure 23a. The mean annual value of net radiation is 216 Watts per square metre but monthly values show a strong seasonal variation. The annual cycle indicates that higher values of solar (net) radiation occur from September to December, just before the monsoon season or during the spring season. The net radiation is relatively low during the peak period of the wet season (January to March), compared to the spring months, presumably suppressed by increased cloudiness during summer. The period of minimum net radiation from April to August coincides with the dry season.

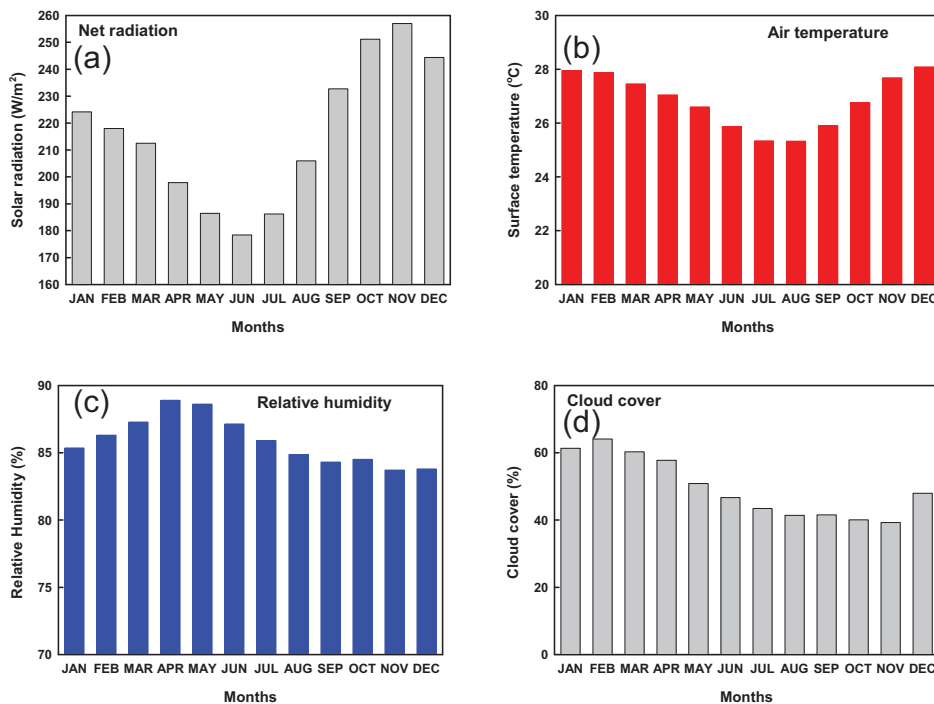


**Figure 23.**(a) Mean monthly values of net radiation, (b) surface temperature at 2 metres, (c) relative humidity at 2 metres and (d) cloud cover in the Torres Strait region. Net radiation units (Watts per square metre), surface temperature (°C) and, relative humidity (%) and cloud cover (%). The region is defined here as the grid between 9-11°S and 141-145°E. Source: NCEP reanalysis.

The mean annual surface temperature is 26.8 °C. Surface temperature shows little variation throughout the year. The period from November to March shows higher values, while other months that coincide with the dry season show lower values (Figure 23b). December is the warmest month with 28.1 °C, while August is the coolest month with 25.3 °C.

Relative humidity is one of the important parameters that affect comfort in the region. The annual average relative humidity is 86% and shows peak values during April and May, after the wet season (Figure 23c). Relative humidity is above 80% throughout the year. Higher temperatures, cloud cover and rainfall with high relative humidity conditions make conditions uncomfortable. This aspect will be discussed in relation to apparent temperature.

The average annual cloud cover over the region is about 50%, but higher values are found during the peak months of the wet season, January to March (Figure 23d), while less than 50% is recorded from June to November.

## 2.2 Regional Sea Surface Temperatures: Mean, Trends and Variability

Sea Surface Temperature (SST) can affect human activities in this region. The ocean is important as a source of food and the basis of several industries (e.g. sea sponge production, fishing, pearl, navigation) Therefore, SST and wind patterns can play an important role in day-to-day life. Annual SST in this region is about 28° C (Figure 24) with small seasonal variations. The period from December to May has higher SSTs (Figure 25), while other months have lower SSTs.

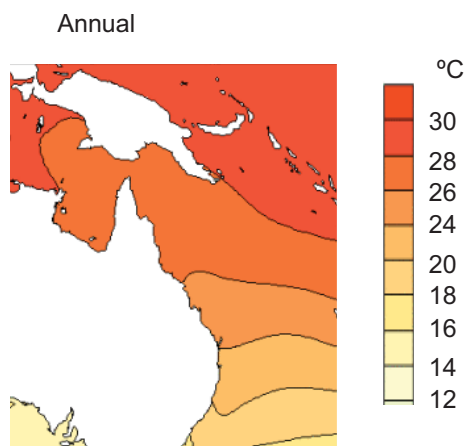


**Figure 24.** Annual sea surface temperature in the Torres Strait region. Source: Australian Bureau of Meteorology.

SSTs derived from larger spatial scales do not indicate local scale variations, but on the other hand, such variations could be minimal over a small area such as the Torres Strait region.

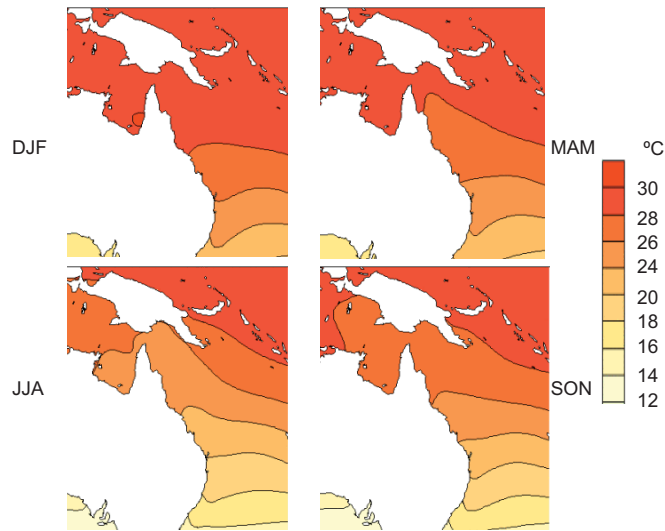


**Figure 25.** Seasonal sea surface temperatures in the Torres Strait region. Source: Australian Bureau of Meteorology.

SSTs over the region have increased by about 0.16 - 0.18 °C per decade from 1950 to present. Such a trend is visible in the annual and seasonal patterns shown in Figure 26. SSTs in the northern tropics, north of Australia and the south of the equator, show an increasing trend with strong inter-annual variability.

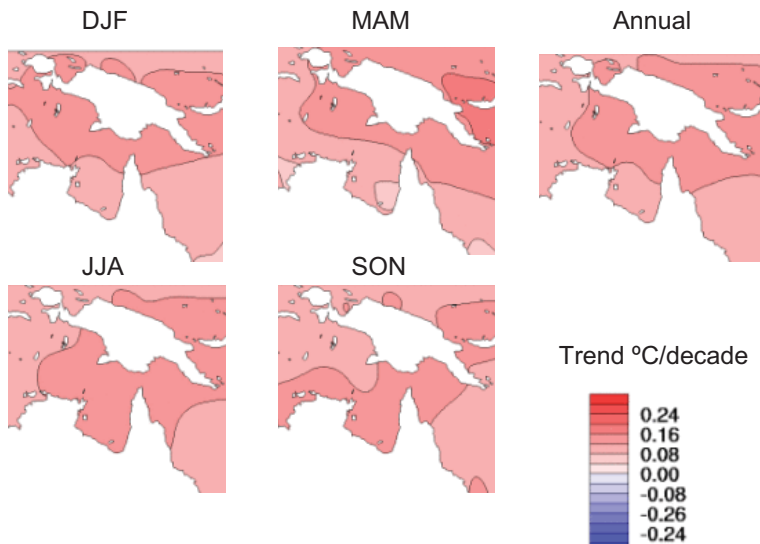


**Figure 26.** Trends in sea surface temperature in the Torres Strait region. Trends are calculated from 1950 to present and shown as °C per decade. Source: Australian Bureau of Meteorology.

Mean wet season average SST for the period between 1961-1990 is 28.3 °C, which is slightly higher than the dry season mean value of 27.4 °C. SST anomalies based on 1961-1990 average values show a greater rise since 1980 during both wet and dry

seasons (Figure 27). These increases can have significant effects on human life in this region.

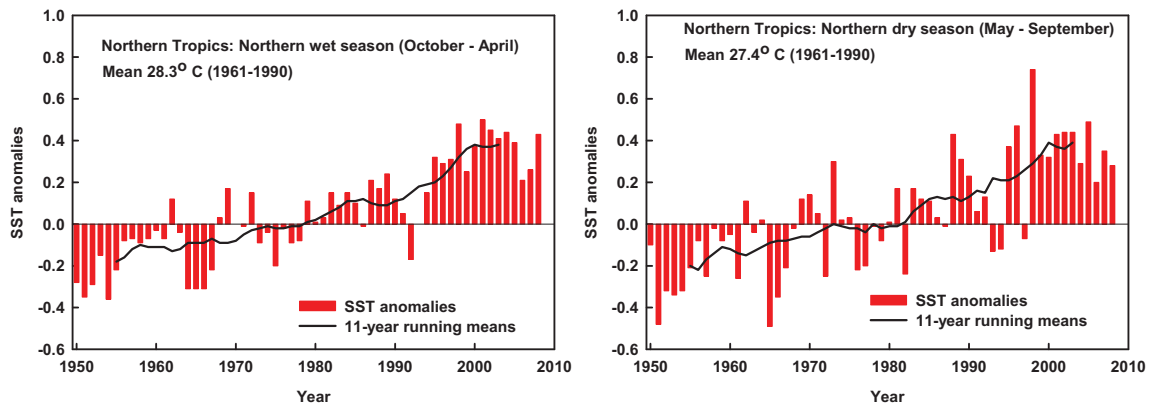


**Figure 27.** Sea surface temperature anomalies (relative to the 1961-1990 mean) for both the northern wet (October-April) and dry (May – September) seasons. Vertical red bars indicate actual anomalies and the black line shows decadal-scale variations and trends. (Source: Australian Bureau of Meteorology).

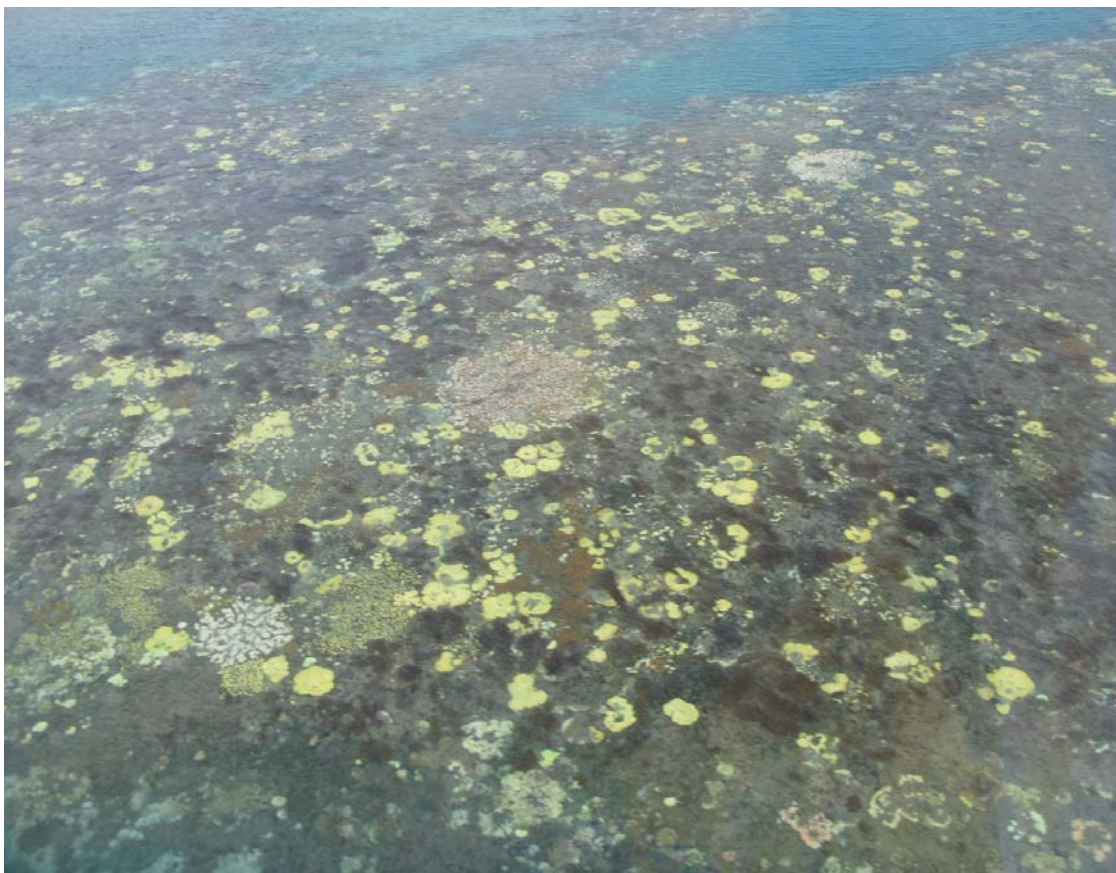


**Photo 7.** Coral bleaching around Thursday Island. (Source Andrew Baird.)

### 2.3 Maximum, minimum and mean temperatures: Trends and variability at Thursday Island and Daru

The annual temperature at Daru is 26.9 °C and on Thursday Island (MO) is 26.8 °C. These values are very close to the annual value derived from Figure 23b, (26.8 °C). As can be seen from Figure 28, variation in temperature throughout the year is minimal (2 to 3 °C) between winter dry and summer wet months. The annual cycle in monthly temperature is negligible as shown in Figure 28. The warmer months are from September to April and cooler months are from May to August.

Annual and seasonal temperature trends and variations of the southern part of the region are shown using data from Thursday Island and Horn Island, while variations and trends in the northern part are shown by using data from Daru. It is evident from Figure 29 that the temperatures at both Thursday Island and Daru show a positive trend during the last 50 years with marked inter-annual variability. The maximum temperature at Thursday Island has increased by 0.32 °C/decade between 1960 and the mid 1990s and by 0.67 °C/decade between the mid 1990s and 2009. Minimum temperature increased by 0.18 °C/decade between 1960 and the mid 1990s and by 0.35 °C/decade between the mid mid-1990s and 2009. Mean temperature increased by 0.25 °C/decade between 1960 and the mid 1990s and by 0.51 °C /decade between the mid-1990s and 2009. Since the latter period is relatively short (14 years) caution is needed when interpreting the results. The northern part of the region (represented by Daru) also shows a positive trend in annual and seasonal temperatures, but the increases are less than those at Thursday Island. Temperatures at these stations show marked inter-annual variability.

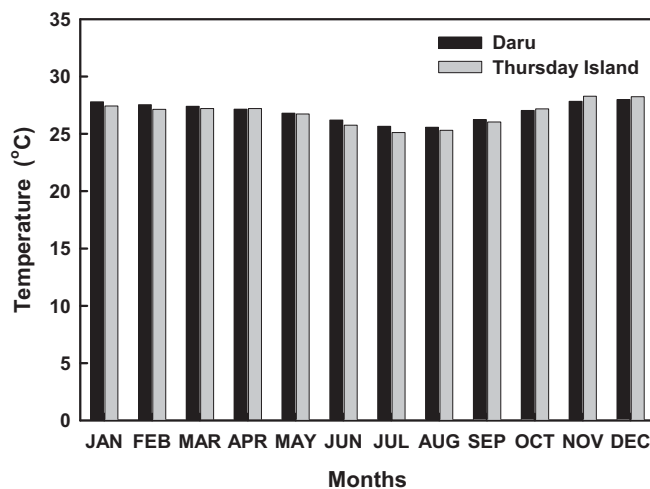


**Figure 28.** Mean monthly temperatures at Daru and Thursday Island.

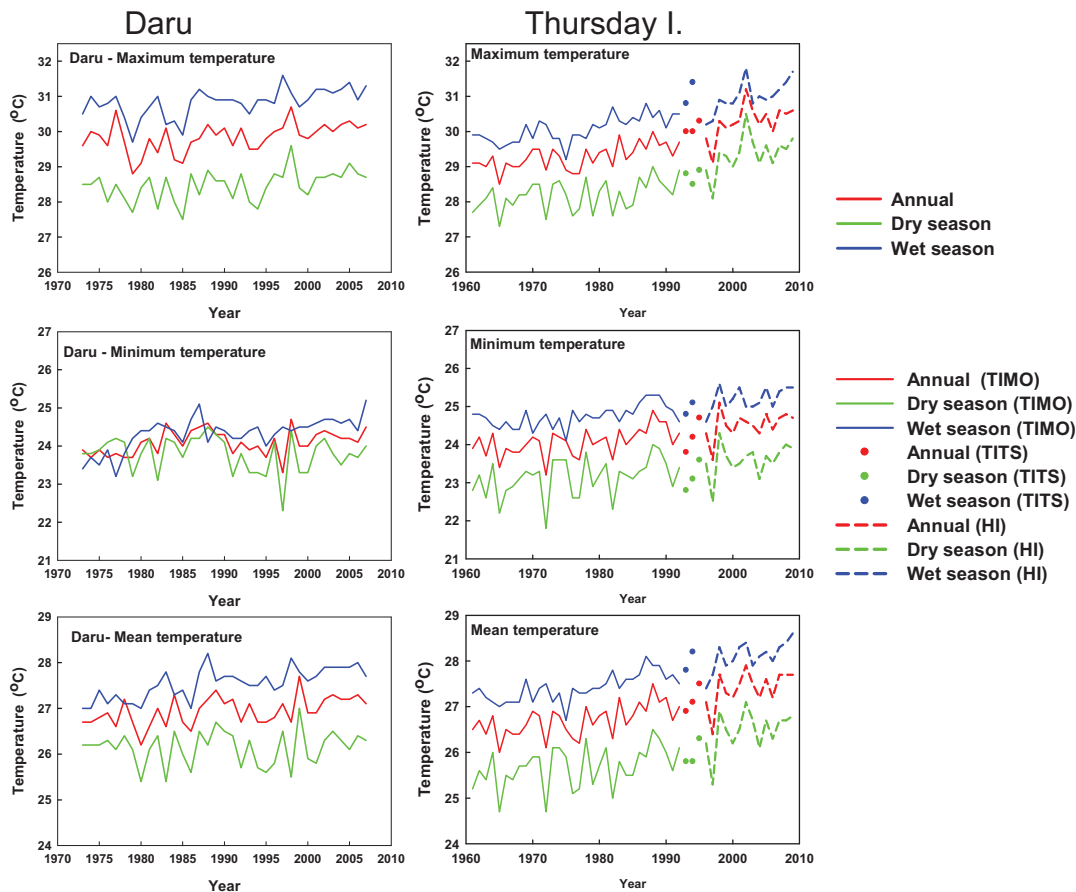


**Figure 29.** Trends and variability in annual (red lines), wet (blue lines) and dry (green lines) seasons temperature at Thursday Island and Daru. TIMO: Thursday Island Met. Office, TITS: Thursday Island Township and HI: Horn Island. Source: Australian Bureau of Meteorology and National Weather Service, Papua New Guinea.

## 2.4 Apparent temperature

The word “apparent” has been used more commonly since about 1980 to refer to how various temperature and humidity combinations feel to humans based on physiology and clothing science. It reflects the need for the body to maintain a thermal equilibrium and particularly applies to the summer months, because relative humidity is much more important to human comfort when air temperatures are above a certain threshold.

In general, temperature and relative humidity are higher and wind speed is weaker, during the wet season. The reverse is generally true during the dry season. When relative humidity is very high in the tropical environment (e.g. above 80 percent) the air can actually feel warmer than the air temperature because of the ability of the body to shed heat through evaporation is reduced (particularly if there is little air movement). On the other hand, when relative humidity is lower, say about 60 percent, the body can feel cooler than the air temperature because the higher rate of evaporation of perspiration cools the skin.

The key variables defining human thermal comfort can be combined into one indicator called the Apparent Temperature (AT). AT is a heat index invented in Australia in the 1970s by Robert Steadman (1984; 1994). The four main environmental factors are wind, temperature, humidity and radiation. Wind and radiation are microclimatic

elements influenced by local factors such as aspect, shelter from wind, shade, nearby surfaces and so on. As such, they are best measured on site, rather than generalized for a region.

The formula used in to calculate AT is:

$$AT = Ta + 0.348 \times e - 0.70 \times ws + 0.70 \times Q / (ws + 10) - 4.25$$

Ta = Dry bulb temperature (°C)

e = Water vapour pressure (hPa) [humidity]

ws = Wind speed (m/s) at an elevation of 10 metres

Q = Net radiation absorbed per unit area of body surface (w/m<sup>2</sup>)

where

$$e = rh / 100 \times 6.105 \times \exp (17.27 \times Ta / (237.7 + Ta))$$

rh = Relative Humidity [%]

Apparent temperatures have been calculated using area-averaged monthly values of net radiation and air temperature at 2 metres, relative humidity at 2 metres and wind speed at 10 metres for individual years, from 1948 to 2009 from NCEP re-analysis. Long-term monthly averages (climatological values) of apparent temperatures were calculated and are shown in Figure 30. If we consider only air temperature and relative humidity, the values are slightly less than those values based on all four variables. This indicates significant contributions of net radiation and wind speed to apparent temperature in the region. The long-term averages for these parameters are shown in Figures 6, 7 and 23. The annual apparent temperature is 38.4 °C and for wet and dry seasons are 42.3 °C and 33.6 °C, respectively. Apparent temperature for the three-month periods of December to February, March to May, June to August and September to November are 43.8 °C, 39.2 °C, 32.5 °C and 38.6 °C. As mentioned earlier, higher temperatures and relative humidity and lower wind speeds and intense solar radiation are important climatic factors during the wet season. Relatively opposite conditions contribute to slightly lower values during the dry season.

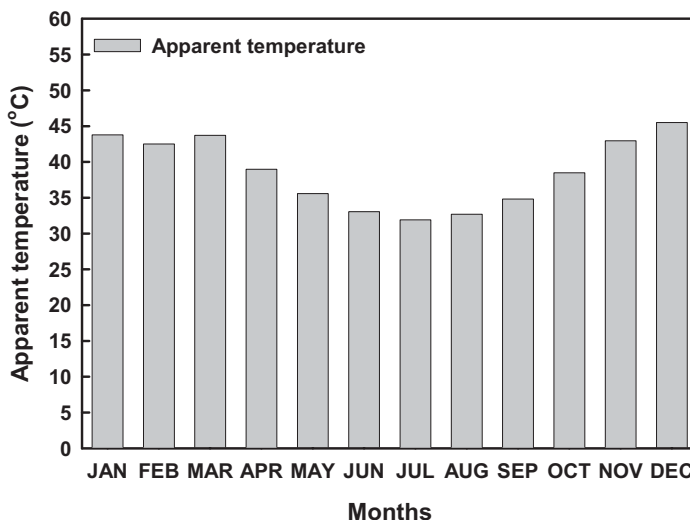


**Figure 30.** Monthly apparent temperatures for the Torres Strait region. The region is defined here as the grid between 9-11°S and 141-145°E. Source: NCEP reanalysis.

Year to year changes in apparent temperature in Figure 31 do not show a clear long-term trend, but the last decade shows a small decrease. However, such a decrease does not contribute much to comfort in the region, as apparent temperatures are always high due to high relative humidity, solar radiation and temperature.

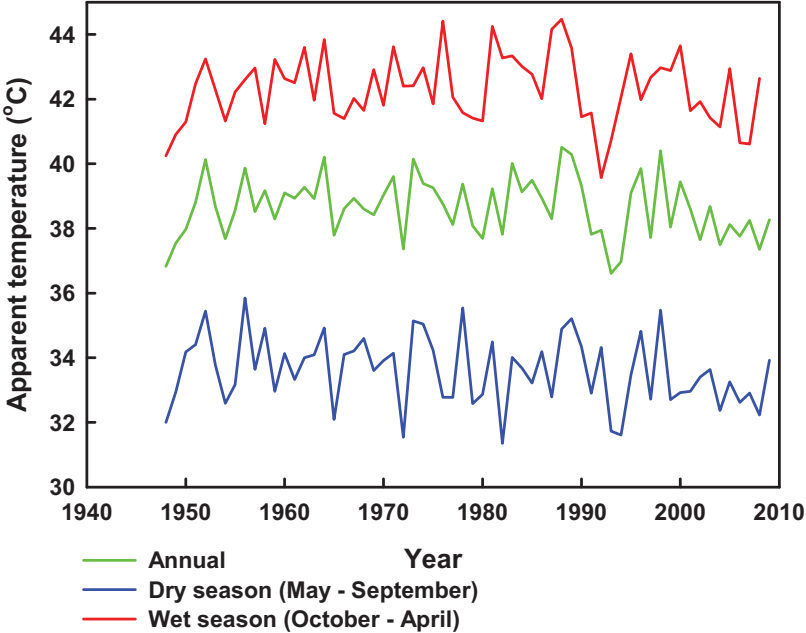


**Figure 31.** Year to year variability in annual, wet and dry season apparent temperatures in the Torres Strait region.

### 3. METHOD FOR GENERATING FUTURE CLIMATES

The CSIRO and Bureau of Meteorology (2007) Technical Report describes in detail the methodology used to synthesize climate model projections for Australia. The same method applies to generating projections at the regional scale.

#### 3.1 Uncertainties associated with future projections.

There are three major uncertainties associated with future climate change projections.

- 1) The uncertainty in the future evolution of greenhouse gas and sulphate aerosol emissions.
- 2) The uncertainty in how much the global average surface temperature will respond to increases in atmospheric greenhouse gas concentrations and changes in sulphate aerosol emissions.
- 3) The uncertainty in how the climate of Australia will respond to an increase in global average surface temperature.

The first uncertainty is addressed by considering six different scenarios for the future evolution of greenhouse gas and sulphate aerosol emissions as described by the Special Report on Emissions Scenarios (SRES) (Nakićenović and Swart, 2000) of the Intergovernmental Panel on Climate Change (IPCC). These emissions scenarios are illustrated in Figure 32. Each of the scenarios, denoted A1B, A1FI, A1T, A2, B1 and B2, is based on a plausible storyline of future global demographic, economic and technological change in the 21<sup>st</sup> Century.

The second uncertainty is addressed by considering information on the response of the global average surface temperature to the emissions scenarios from multiple climate models. This is reported in the IPCC's Fourth Assessment Report IPCC (2007) and Meehl *et al.* (2007b). This is summarized in Figure 33, which shows projected changes in global average surface temperature for the six scenarios. Warmings, relative to the average temperature for the 1980-2000 period, of between 0.5 and 1.6 °C by 2030 and between 1.1 and 6.4 °C by 2100 are suggested. This Figure also shows that simulated global average surface temperature anomalies for the 20<sup>th</sup> Century agree well with observed anomalies on the timescale of several decades, giving us some confidence in the ability of climate models to accurately simulate anomalies on such a timescale.

A more recent study by Reisinger *et al.* (2010) suggests that uncertainties in the Global Warming Potential (GWP) of major greenhouse gases (CO<sub>2</sub> and CH<sub>4</sub>) now appear significantly larger than indicated by the IPCC assessments. In their study, first they presented a comprehensive evaluation of uncertainties in the Global Warming Potential (GWP) and Global Temperature Change Potential (GTP) of CH<sub>4</sub>, using a simple climate model calibrated to Atmosphere-Ocean Global Climate Models (AOGCMs) and coupled climate-carbon cycle models assessed in the IPCC Fourth Assessment Report (AR4). In addition, they estimated uncertainties in these metrics probabilistically by using a method that does not rely on AOGCMs but instead builds on

historical constraints and uncertainty estimates of current radiative forcings. While their mean and median GWPs and GTPs estimates are consistent with previous studies, their analysis suggests that uncertainty ranges for GWPs are almost twice as large as estimated in the AR4. Relative uncertainties for GTPs are larger than for GWPs, nearly twice as high for a time horizon of 100 years. Given this uncertainty, they suggested the possibility for substantial future adjustments in best-estimate values of GWPs and in particular GTPs

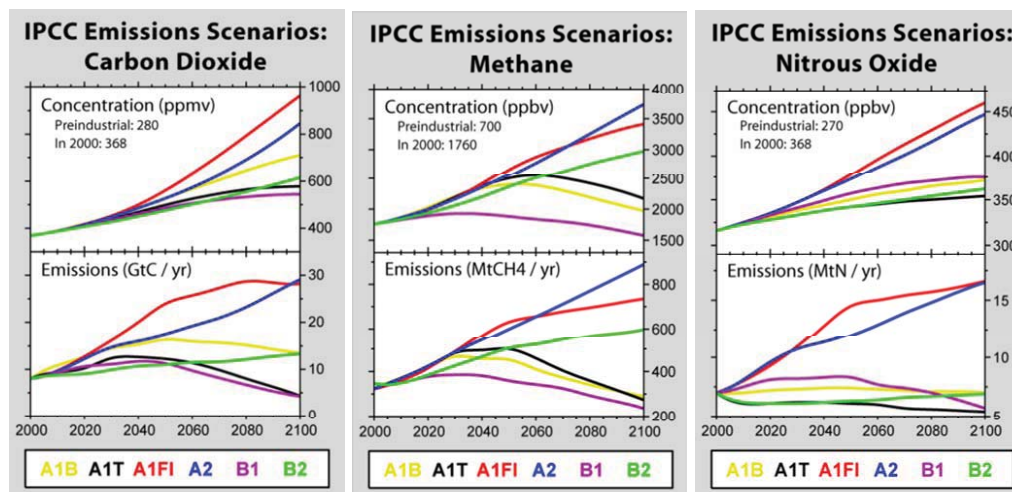


**Figure 32.** Atmospheric concentrations and emissions of carbon dioxide, methane and nitrous oxide for six SRES scenarios. Source: Nakićenović and Swart (2000).

For each period of interest and each scenario, the range of warming is described using a probability distribution, which comprises a set of probabilities assigned to the numerous plausible values of change.

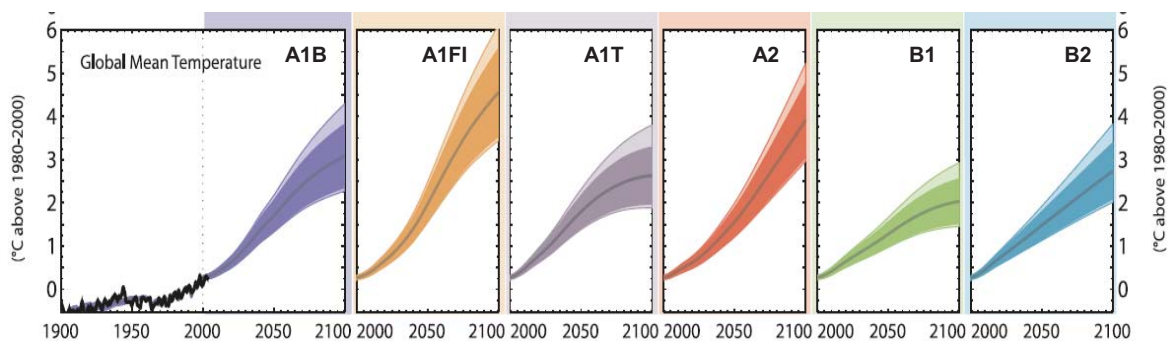


**Figure 33.** Changes, relative to the average for the period 1980-2000 in global average surface temperature for the 21<sup>st</sup> Century for the A1B, A1FI, A1T, A2, B1 and B2 SRES emissions scenarios. The dark shaded areas represent uncertainties in changes based on the consideration of the response of 19 climate models to the emissions scenarios. The light shaded areas represent uncertainties in changes based on the consideration of the response of the models to the emissions scenarios and uncertainty in carbon cycle feedbacks in the climate system. The coloured lines indicate changes based on the mean average response of the models and mid-range assumptions about carbon cycle feedbacks. The black line indicates changes recorded during the 20<sup>th</sup> Century. Source: Meehl et al. (2007b).

The third uncertainty is addressed by considering the response of the climate of Australia to global warming in 24 climate models. Model outputs from the Coupled Model Inter-comparison Project phase 3 (CMIP3) multi-model dataset (see Meehl *et al.*, 2007a) of the World Climate Research Programme (WCRP) were processed using the pattern scaling technique described by Mitchell *et al.* (1999), Mitchell (2003) and Whetton *et al.* (2005). From the simulations of the 21<sup>st</sup> century from each model, the trend in each variable and each model grid point was calculated, relative to the global mean warming. The results from the 24 models were then combined to form a probability distribution for local change per degree of warming. In this process, models were given differing weights, or emphasis, depending on their ability to simulate average patterns of temperature, precipitation and mean sea level pressure in the Australian region for the 30-year period, 1961-1990.

CSIRO has access to simulated monthly data for 12 climate variables, from up to 24 global climate models (some models provide all variables, but not all) from 1900-2100 for three emission scenarios (A1B, A2 and B1; for emission scenarios, see Figure 27). We can also scale some results for the highest emission scenario (A1FI), as the global average temperature increase is tracking the A1FI emission scenario. Typically, (as in this report) projections are created for individual climate variables, for selected years and emissions scenarios. Projections from different climate models are often mixed together (an ensemble) and expressed as a range of values to represent the uncertainty, *e.g.* a warming of 1-2 °C and a rainfall decrease of 5-10% by 2030. This is suitable for general communication, but it is not suitable for risk assessments involving multiple variables, *e.g.* it would be inappropriate to combine a 1 °C warming with a 10% decrease in rainfall if none of the models simulated this combination. Details of the performance of the models over the Australian region are given in Suppiah *et al.* (2007) and Smith and Chandler (2010). The weightings for the models follow the method provided of Watterson (2008).

## 4. CLIMATE CHANGE PROJECTIONS

This section provides climate change projections in seasonal and annual average downward solar radiation, maximum, minimum and mean temperatures, rainfall, relative humidity and wind speed and evaporation for the years 2030, 2050 and 2070 for A2 and A1FI emission scenarios for the Torres Strait Region. Changes are given for 20-year periods centred on 2030, 2050 and 2070, relative to 30-year averages of the period, 1975-2004. Conditions in any individual year will be strongly affected by natural climate variability (variability on inter-annual to decadal scales is not easily predicted and has not been accounted for).

Seasons are defined as summer (December to February, abbreviated to DJF), autumn (March to May, MAM), winter (June to August, JJA) and spring (September to November, SON). The best estimates are shown as the median (the 50<sup>th</sup> percentile) and lower and upper ranges are shown as 10<sup>th</sup> and 90<sup>th</sup> percentiles of the ensemble. The region is defined here as the grid between 9-11°S and 141-145°E.

### 4.1 Projected changes in solar radiation and temperature

Table 1 shows changes in annual and seasonal downward solar radiation for the region for 2030, 2050 and 2070 for A2 and A1FI emission scenarios. Changes indicate decreases and increases, but decreases dominate the overall median (indicated by the 50<sup>th</sup> percentile) pattern in the future. The annual change for 2030 is -0.31%, but slightly larger decreases are projected for 2050 and 2070 for the A2 emission scenario. Larger changes are also projected for the higher emission scenario (A1FI). Seasonal changes are also dominated by decreases.

*Table 1. Projected changes in solar radiation (%) for A2 and (b) A1FI emission scenarios for 2030, 2050 and 2070. Changes are based on simulations from 22 models.*

(a) SRES A2 Downward solar radiation (%)

Year	2030			2050			2070		
Percentiles	10 <sup>th</sup>	50 <sup>th</sup>	90 <sup>th</sup>	10 <sup>th</sup>	50 <sup>th</sup>	90 <sup>th</sup>	10 <sup>th</sup>	50 <sup>th</sup>	90 <sup>th</sup>
DJF	-1.72	-0.24	1.17	-2.93	-0.42	1.99	-4.12	-0.63	2.85
MAM	-1.50	-0.28	0.96	-2.63	-0.48	1.67	-3.83	-0.78	2.66
JJA	-0.97	-0.45	1.08	-1.65	-0.77	1.89	-2.30	-0.90	2.96
SON	-1.57	-0.39	0.21	-2.70	-0.67	0.37	-3.98	-1.01	0.57
Annual	-1.18	-0.31	0.82	-2.01	-0.54	1.41	-2.79	-0.79	2.09

(b) SRES A1FI Downward solar radiation (%)

Year	2030			2050			2070		
Percentiles	10 <sup>th</sup>	50 <sup>th</sup>	90 <sup>th</sup>	10 <sup>th</sup>	50 <sup>th</sup>	90 <sup>th</sup>	10 <sup>th</sup>	50 <sup>th</sup>	90 <sup>th</sup>
DJF	-2.04	-0.19	1.28	-3.48	-0.33	2.24	-4.89	-0.53	3.35
MAM	-1.77	-0.37	1.10	-3.10	-0.64	1.93	-4.50	-0.95	3.10
JJA	-1.14	-0.42	1.24	-1.94	-0.71	2.17	-2.71	-1.05	3.48
SON	-1.52	-0.46	0.19	-2.60	-0.79	0.33	-4.12	-1.24	0.54
Annual	-1.39	-0.43	0.81	-2.36	-0.74	1.42	-3.29	-1.10	2.28

The Torres Strait region is expected to warm in response to increases in global average surface temperature. Table 2 shows annual and seasonal increases in maximum, minimum and mean temperatures for 2030, 2050 and 2070 for A2 and A1FI emission scenarios. Increases in temperature by 2030 do not show large differences between these two emission scenarios, but differences are large for 2050 and 2070. Annual mean temperature in the region increases by 0.87 °C with a range between 0.62 and 1.08 °C by 2030 for the A2 emission scenario. Under the A1FI emission scenario, annual mean temperature increases by 1.02 °C with a range between 0.73 and 1.27 °C by 2030. Higher increases are projected for 2050 and 2070 depending upon the emission scenario. Increases in maximum and minimum do not necessarily match the mean temperature increase as there are differences in the number of models used for maximum and minimum temperatures and mean temperatures. Annual maximum temperature increases by 0.73 °C with a range 0.55 to 1.10 °C and minimum temperature increases by 0.79 °C with a range 0.55 to 1.05 °C by 2030 under the A2 emission scenario. Larger increases are projected for 2050 and 2070 and also for the A1FI emission scenario.

*Table 2. Changes in maximum, minimum and mean temperatures for A2 (a to c) and A1FI (d to f) emission scenarios for 2030, 2050 and 2070. Results from 8 models have been used to construct projections for maximum and minimum temperatures and from 24 models for mean temperature.*

(a) SRES A2 Maximum temperature (°C)

Year	2030			2050			2070		
Percentiles	10 <sup>th</sup>	50 <sup>th</sup>	90 <sup>th</sup>	10 <sup>th</sup>	50 <sup>th</sup>	90 <sup>th</sup>	10 <sup>th</sup>	50 <sup>th</sup>	90 <sup>th</sup>
DJF	0.56	0.72	1.08	0.98	1.23	1.85	1.55	1.72	2.67
MAM	0.56	0.73	1.15	0.98	1.24	1.98	1.55	1.78	2.86
JJA	0.55	0.76	1.13	0.95	1.28	1.94	1.50	1.79	2.81
SON	0.52	0.73	1.05	0.90	1.24	1.80	1.38	1.75	2.60
Annual	0.55	0.73	1.10	0.95	1.25	1.88	1.50	1.76	2.72

(b) SRES A2 Minimum temperature (°C)

Year	2030			2050			2070		
Percentiles	10 <sup>th</sup>	50 <sup>th</sup>	90 <sup>th</sup>	10 <sup>th</sup>	50 <sup>th</sup>	90 <sup>th</sup>	10 <sup>th</sup>	50 <sup>th</sup>	90 <sup>th</sup>
DJF	0.58	0.77	1.03	1.02	1.32	1.77	1.60	1.90	2.55
MAM	0.59	0.78	1.09	1.03	1.33	1.86	1.63	1.92	2.68
JJA	0.53	0.81	1.09	0.93	1.37	1.87	1.47	1.92	2.70
SON	0.50	0.81	1.02	0.87	1.39	1.75	1.38	2.00	2.54
Annual	0.55	0.79	1.05	0.96	1.35	1.80	1.52	1.93	2.60

(c) SRES A2 Mean temperature (°C)

Year	2030			2050			2070		
Percentiles	10 <sup>th</sup>	50 <sup>th</sup>	90 <sup>th</sup>	10 <sup>th</sup>	50 <sup>th</sup>	90 <sup>th</sup>	10 <sup>th</sup>	50 <sup>th</sup>	90 <sup>th</sup>
DJF	0.64	0.86	1.12	1.11	1.46	1.90	1.70	2.08	2.65
MAM	0.65	0.88	1.09	1.13	1.49	1.85	1.74	2.12	2.58
JJA	0.60	0.81	1.14	1.04	1.38	1.93	1.60	1.97	2.69
SON	0.57	0.83	1.06	0.98	1.42	1.81	1.49	2.00	2.52
Annual	0.62	0.87	1.08	1.08	1.48	1.83	1.65	2.07	2.56

(d) SRES A1FI Maximum temperature (°C)

Year	2030			2050			2070		
Percentiles	10 <sup>th</sup>	50 <sup>th</sup>	90 <sup>th</sup>	10 <sup>th</sup>	50 <sup>th</sup>	90 <sup>th</sup>	10 <sup>th</sup>	50 <sup>th</sup>	90 <sup>th</sup>
DJF	0.66	0.89	1.35	1.15	1.52	2.30	1.78	2.12	3.25
MAM	0.66	0.91	1.45	1.15	1.55	2.47	1.78	2.16	3.49
JJA	0.66	0.91	1.42	1.14	1.55	2.42	1.76	2.15	3.42
SON	0.64	0.89	1.38	1.10	1.51	2.34	1.61	2.10	3.26
Annual	0.65	0.90	1.38	1.12	1.53	2.35	1.74	2.13	3.31

(e) SRES A1FI Minimum temperature (°C)

Year	2030			2050			2070		
Percentiles	10 <sup>th</sup>	50 <sup>th</sup>	90 <sup>th</sup>	10 <sup>th</sup>	50 <sup>th</sup>	90 <sup>th</sup>	10 <sup>th</sup>	50 <sup>th</sup>	90 <sup>th</sup>
DJF	0.69	0.97	1.29	1.19	1.65	2.20	1.85	2.30	3.10
MAM	0.70	1.00	1.36	1.21	1.69	2.32	1.88	2.35	3.28
JJA	0.62	0.99	1.36	1.09	1.68	2.33	1.69	2.34	3.29
SON	0.59	1.02	1.28	1.02	1.73	2.18	1.58	2.40	3.04
Annual	0.65	0.98	1.31	1.13	1.67	2.24	1.75	2.33	3.16

(f) SRES A1FI Mean temperature (°C)

Year	2030			2050			2070		
Percentiles	10 <sup>th</sup>	50 <sup>th</sup>	90 <sup>th</sup>	10 <sup>th</sup>	50 <sup>th</sup>	90 <sup>th</sup>	10 <sup>th</sup>	50 <sup>th</sup>	90 <sup>th</sup>
DJF	0.75	1.01	1.32	1.30	1.72	2.24	2.00	2.45	3.12
MAM	0.77	1.03	1.28	1.33	1.76	2.18	2.04	2.50	3.03
JJA	0.71	0.95	1.34	1.23	1.62	2.27	1.88	2.32	3.17
SON	0.67	0.98	1.25	1.15	1.67	2.13	1.76	2.35	2.96
Annual	0.73	1.02	1.27	1.27	1.74	2.16	1.94	2.44	3.01

## 4.2 Projected changes in rainfall, relative humidity and wind speed

The pattern of rainfall change is more complex than that for temperature, and includes both increases and decreases. Model to model variations in rainfall simulations are also large. Table 3 shows annual and seasonal changes in rainfall, relative humidity and wind speed in the region for 2030, 2050 and 2070 for the A2 and A1FI emission scenarios. In general, the models suggest a small increase in rainfall in the region as shown by the 50<sup>th</sup> percentile. However, changes in rainfall show both decreases and increases. The best estimate for the annual rainfall change by 2030 for A2 emission scenario is 1.24% with a range between -2.97 and 5.33%. Increases are slightly higher for DJF, MAM and SON than for JJA. The annual increase by 2030 for A1FI emission scenario is 1.46% with a range between -3.49 and 6.27%. Moderate increases in best estimates and larger ranges are projected for 2050 and 2070. Ranges become larger for JJA and SON by 2070, both in A2 and A1FI emission scenarios.

As mentioned in the previous section 2.1, this region has high relative humidity throughout the year and this is a critical factor for human comfort. Under climate change conditions, relative humidity is expected to change little in the region with projected changes of between -1 and +1% (Table 3 (c and d)). The annual change in relative humidity by 2030 for the A2 emission scenario is -0.04% with a range between -0.58 and 0.20% and for the A1FI emission scenario is -0.05% with a range between -0.69 and 0.23%. The projected changes remain small for 2050 and 2070.

Table 3. Projected changes in rainfall (a and b), relative humidity (c and d) and wind speed (e and f) for SRES A2 and A1FI emission scenarios for 2030, 2050 and 2070. Changes in all three variables are shown in percentage. Simulations of 24 models were used in projecting rainfall, 13 models for relative humidity and 19 models for wind speed.

(a) SRES A2 Rainfall (%)

Year	2030			2050			2070		
Percentiles	10 <sup>th</sup>	50 <sup>th</sup>	90 <sup>th</sup>	10 <sup>th</sup>	50 <sup>th</sup>	90 <sup>th</sup>	10 <sup>th</sup>	50 <sup>th</sup>	90 <sup>th</sup>
DJF	-2.25	1.31	5.19	-3.82	2.28	9.01	-5.31	3.55	13.94
MAM	-2.68	1.58	7.23	-4.59	2.76	12.39	-6.70	4.16	19.11
JJA	-4.71	0.34	7.85	-8.12	0.57	13.34	-12.14	0.79	18.54
SON	-7.26	1.12	8.51	-12.59	1.97	14.89	-19.73	3.16	23.93
Annual	-2.97	1.24	5.33	-5.09	2.14	9.19	-7.57	3.21	14.09

(b) SRES A1FI Rainfall (%)

Year	2030			2050			2070		
Percentiles	10 <sup>th</sup>	50 <sup>th</sup>	90 <sup>th</sup>	10 <sup>th</sup>	50 <sup>th</sup>	90 <sup>th</sup>	10 <sup>th</sup>	50 <sup>th</sup>	90 <sup>th</sup>
DJF	-2.64	1.54	6.11	-4.49	2.68	10.60	-6.25	4.18	16.40
MAM	-3.15	1.85	8.50	-5.40	3.24	14.58	-7.89	4.90	22.48
JJA	-5.54	0.39	9.23	-9.55	0.67	15.69	-14.29	0.93	21.82
SON	-8.54	1.32	10.01	-14.82	2.31	17.52	-23.22	3.72	28.15
Annual	-3.49	1.46	6.27	-5.99	2.52	10.81	-8.90	3.78	16.57

(c) SRES A2 Relative humidity (%)

Year	2030			2050			2070		
Percentiles	10 <sup>th</sup>	50 <sup>th</sup>	90 <sup>th</sup>	10 <sup>th</sup>	50 <sup>th</sup>	90 <sup>th</sup>	10 <sup>th</sup>	50 <sup>th</sup>	90 <sup>th</sup>
DJF	-0.46	-0.16	0.18	-0.79	-0.27	0.31	-1.10	-0.38	0.48
MAM	-0.60	0.05	0.18	-1.02	0.09	0.31	-1.41	0.12	0.49
JJA	-0.69	0.04	0.23	-1.17	0.06	0.40	-1.63	0.09	0.55
SON	-0.66	-0.01	0.18	-1.13	-0.01	0.31	-1.60	-0.02	0.49
Annual	-0.58	-0.04	0.20	-0.99	-0.08	0.34	-1.38	-0.11	0.48

(d) SRES A1FI Relative humidity

Year	2030			2050			2070		
Percentiles	10 <sup>th</sup>	50 <sup>th</sup>	90 <sup>th</sup>	10 <sup>th</sup>	50 <sup>th</sup>	90 <sup>th</sup>	10 <sup>th</sup>	50 <sup>th</sup>	90 <sup>th</sup>
DJF	-0.55	-0.19	0.21	-0.93	-0.32	0.36	-1.29	-0.45	0.57
MAM	-0.70	0.06	0.21	-1.19	0.10	0.37	-1.66	0.14	0.58
JJA	-0.81	0.04	0.28	-1.38	0.07	0.47	-1.92	0.10	0.65
SON	-0.78	-0.01	0.21	-1.33	-0.02	0.37	-1.88	-0.02	0.57
Annual	-0.69	-0.05	0.23	-1.17	-0.09	0.40	-1.63	-0.12	0.56

(e) SRES A2 Wind speed (%)

Year	2030			2050			2070		
Percentiles	10 <sup>th</sup>	50 <sup>th</sup>	90 <sup>th</sup>	10 <sup>th</sup>	50 <sup>th</sup>	90 <sup>th</sup>	10 <sup>th</sup>	50 <sup>th</sup>	90 <sup>th</sup>
DJF	-3.25	0.91	3.88	-5.54	1.57	6.62	-7.77	2.31	9.59
MAM	-2.47	0.70	2.34	-4.21	1.21	4.03	-5.93	1.78	5.92
JJA	-1.04	0.28	0.91	-1.77	0.47	1.56	-2.47	0.63	2.29
SON	-0.24	0.39	2.26	-0.42	0.67	3.88	-0.69	0.97	5.70
Annual	-0.95	0.34	1.72	-1.62	0.59	2.96	-2.31	0.74	4.96

(f) SRES A1FI Wind speed (%)

Year	2030			2050			2070		
Percentiles	10 <sup>th</sup>	50 <sup>th</sup>	90 <sup>th</sup>	10 <sup>th</sup>	50 <sup>th</sup>	90 <sup>th</sup>	10 <sup>th</sup>	50 <sup>th</sup>	90 <sup>th</sup>
DJF	-3.83	1.34	5.49	-6.51	2.27	9.33	-9.14	3.16	12.98
MAM	-2.91	0.92	3.54	-4.95	1.56	6.02	-6.98	2.18	8.37
JJA	-1.23	0.58	1.43	-2.08	0.99	2.43	-2.90	1.38	3.38
SON	-0.13	1.11	3.48	-0.21	1.89	5.92	-0.30	2.63	8.24
Annual	-1.12	0.37	2.47	-1.91	0.63	4.19	-2.72	0.87	5.84

Changes in annual wind speed are also small as shown in Table 3 (e and f). The best estimate for annual wind speed change by 2030 for the A2 emission scenario is 0.34% with a range between -0.95 and 1.72%. For the A1FI emission scenario, the annual change is 0.37% with a range between -1.12 and 2.47%. A very small increase has been projected in annual values for 2050 and 2070 for the two emission scenarios. However, there are some differences in wind speed projections among the seasons. Although the wind speed increases in all seasons, DJF, MAM and SON show slightly higher values than JJA for the two scenarios and for 2050 and 2070.

### 4.3 Projected changes in potential evaporation

Future changes in annual and seasonal potential evaporation and their ranges for the region are shown in Table 4. Overall there is an increase in potential evaporation in the future and the increase is even more for the A1FI emission scenario. The best estimate of annual increase by 2030 for the A2 emission scenario is 2.63% with a range between 1.94 and 4.72%. For the A1FI emission scenario, the annual increase by 2030 is 3.74% with a range between 2.28 and 5.87%. Larger increases and ranges are projected for 2050 and 2070 for the two emission scenarios.

Table 4. Projected changes (%) in potential evaporation for (a) A2 and (b) A1FI emission scenarios for 2030, 2050 and 2070 from 13 models.

(a) SRES A2 Evaporation (%)

Year	2030			2050			2070		
Percentiles	10 <sup>th</sup>	50 <sup>th</sup>	90 <sup>th</sup>	10 <sup>th</sup>	50 <sup>th</sup>	90 <sup>th</sup>	10 <sup>th</sup>	50 <sup>th</sup>	90 <sup>th</sup>
DJF	1.26	2.60	4.98	2.14	4.50	8.47	2.98	6.26	11.87
MAM	1.87	3.18	4.95	3.21	5.47	8.51	4.72	8.08	12.72
JJA	2.61	3.06	5.70	4.45	5.20	9.81	6.26	8.05	14.64
SON	2.03	2.37	3.99	3.50	4.07	6.80	5.22	5.66	10.03
Annual	1.94	2.63	4.72	3.37	4.53	8.11	4.96	6.69	11.97

(b) SRES A1FI Evaporation (%)

Year	2030			2050			2070		
Percentiles	10 <sup>th</sup>	50 <sup>th</sup>	90 <sup>th</sup>	10 <sup>th</sup>	50 <sup>th</sup>	90 <sup>th</sup>	10 <sup>th</sup>	50 <sup>th</sup>	90 <sup>th</sup>
DJF	1.48	3.28	5.88	2.52	5.58	10.01	3.50	8.11	14.40
MAM	2.37	4.20	6.35	4.02	7.15	10.87	5.60	9.95	15.78
JJA	3.11	3.60	7.17	5.29	6.12	12.28	7.37	9.60	17.77
SON	2.52	2.81	4.92	4.32	4.81	8.42	6.32	6.86	12.19
Annual	2.28	3.74	5.87	3.96	6.35	10.05	5.84	8.84	14.54

### 4.4 Projected changes in apparent temperature

Apparent temperatures (see section 2.4) show that this region has higher values due to its location in the tropics. With the exception of winter (32.5 °C) all seasons show greater than 38 °C, an uncomfortable temperature for humans. The observed annual and seasonal values of solar radiation, mean temperature, wind speed and humidity were modified by the relevant projected changes. There is a clear increase in apparent temperature both annually and in all seasons (see Table 5). These increases are mainly due to larger increases in air temperature and to some extent in wind speed. Changes in solar radiation and relative humidity are small, but as we noted, these variables are relatively high due to the tropical location of the region. Projected

increases in the average annual apparent temperature for the A2 emission scenario by 2030 is 1.32 °C with a range of uncertainty of 0.87 to 1.70 °C and for the A1FI emission scenario is 1.56 °C with a range of uncertainty of 1.03 to 1.96 °C. Best annual estimates of the apparent temperature are 2.29 and 3.24 °C for 2030 and 2050 for the A2 scenario and 2.70 and 3.82 °C for the A1FI emission scenario. Larger increases and ranges are projected for 2050 and 2070 for these emission scenarios. The increases are 2 and 4% for 2030 for the A2 and A1FI emission scenarios. The increases are 6 and 7% by 2050 and 8 and 10% by 2070 for A2 and A1FI emission scenarios. Increases for DJF, MAM and SON are greater than for JJA (Table 5). Ranges are larger around 2070 especially under the A1FI emission scenario.

*Table 5. Projected increases in apparent temperatures for SRES (a) A2 and (b) A1FI emission scenarios for 2030, 2050 and 2070. Changes are shown in percentage.*

(a) SRES A2 Apparent temperature (°C)

Year	2030			2050			2070		
Percentiles	10 <sup>th</sup>	50 <sup>th</sup>	90 <sup>th</sup>	10 <sup>th</sup>	50 <sup>th</sup>	90 <sup>th</sup>	10 <sup>th</sup>	50 <sup>th</sup>	90 <sup>th</sup>
DJF	0.97	1.30	1.77	1.71	2.24	3.04	2.66	3.22	4.29
MAM	1.01	1.36	1.73	1.77	2.34	2.98	2.76	3.35	4.22
JJA	0.93	1.26	1.86	1.60	2.14	3.16	2.47	3.08	4.45
SON	0.69	1.25	1.54	1.20	2.16	2.67	1.87	3.06	3.74
Annual	0.87	1.32	1.70	1.55	2.29	2.92	2.43	3.24	4.08

(b) SRES A1FI Apparent temperature (°C)

Year	2030			2050			2070		
Percentiles	10 <sup>th</sup>	50 <sup>th</sup>	90 <sup>th</sup>	10 <sup>th</sup>	50 <sup>th</sup>	90 <sup>th</sup>	10 <sup>th</sup>	50 <sup>th</sup>	90 <sup>th</sup>
DJF	1.14	1.53	2.03	2.01	2.65	3.51	3.14	3.81	4.98
MAM	1.20	1.59	1.98	2.10	2.76	3.44	3.25	3.96	4.89
JJA	1.10	1.46	2.15	1.89	2.48	3.67	2.90	3.57	5.20
SON	0.83	1.42	1.75	1.45	2.45	3.03	2.23	3.48	4.28
Annual	1.03	1.56	1.96	1.84	2.70	3.39	2.87	3.82	4.81

## 5. CONCLUSIONS

This report is prepared by CSIRO Marine and Atmospheric Research for the Land and Sea Management Unit of the Torres Strait Regional Authority (TSRA). It provides information on the main drivers that dominate most of the observed variability and trends in climate of the past century. This report also provides climate change projections for various climate variables based on simulations conducted for the Fourth Assessment Report of the Intergovernmental Panel on Climate Change.

### 5.1 Observed and projected climates in the Torres Strait region

**Temperature:** The annual average air temperature is about 26.8 °C. December is the warmest month with 28.1 °C, while August is the coolest month with 25.3 °C. The maximum and minimum temperatures increased by 0.32 °C and 0.18 °C per decade between 1960 and the mid 1990s. From the mid 1990s to 2009, maximum and minimum temperatures increased by 0.67 °C and 0.35 °C per decade. The mean temperature increased by 0.25 °C per decade between 1960 and the mid 1990s and by 0.51 °C per decade from the mid 1990s and 2009. The best estimate regional annual average temperature increase by 2030 is 0.87 °C with a range of uncertainty of 0.62 to 1.08 °C for the A2 emission scenario. For the A1FI emission scenario the annual increase by 2030 is 1.02 °C with the range of uncertainty 0.73 to 1.27 °C. Larger increases are projected for 2050 and 2070 for these emission scenarios.

**Sea surface temperature (SST):** The average annual SST in the region is about 28.0 °C and shows small variations throughout the year. The long-term average SST for the wet season is 28.3 °C and for the dry season is 27.4 °C. The average annual and seasonal SSTs in the region have risen by about 0.16 to 0.18 °C per decade from 1950 to present. Average SSTs in the Great Barrier Reef have significantly warmed since the end of the 19<sup>th</sup> century with the average temperature for the most recent 30 years (1976-2005) is 0.4°C warmer than the earliest instrumental 30 years (1871-1900) (Lough, 2007). The trend in SST for the region, as well as in the Great Barrier Reef, is likely to be continued as the current GCMs are predicting an increase under enhanced greenhouse conditions (Figure 2.12 Lough, 2007).

**Apparent temperature:** The annual apparent temperature is 38.4 °C which is much higher than the annual air temperature of 26.8 °C. The average wet season apparent temperature is 43.8 °C and for the dry season is 33.6 °C. Higher apparent temperature is a result of higher relative humidity, more intense solar radiation and relatively weaker winds during the wet season (and vice versa for the dry season). The projected increase in the average annual apparent temperature for the A2 emission scenario by 2030 is 1.32 °C with a range of uncertainty of 0.87 to 1.70°C and for the A1FI emission scenario is 1.56 °C with a range of uncertainty of 1.03 to 1.96°C. Best annual estimates of the apparent temperature are increases of 2.29 and 3.24°C for 2030 and 2050 for the A2 scenario and 2.70 and 3.82°C for the A1FI emission scenario. Larger increases and ranges are projected for 2050 and 2070 for these emission scenarios.

**Rainfall:** Rainfall shows strong variations on intra-seasonal, inter-annual and inter-decadal time scales. Wet season rainfall dominates the variability with an average amount of 1750 mm between October and April. The dry season (May to September) receives only about 90 mm. Intra-seasonal variation is phase-locked to the seasonal cycle and exists during the Australian monsoon season. Projected rainfall changes include both increases and decreases, but increases dominate overall changes. The best estimate of regional average annual rainfall change for the A2 emission scenario for 2030 is +1.24% with a range of uncertainty of -2.97 to + 5.33%. For the A1FI emission scenario, the best estimate for 2030 is +1.46% with the range of uncertainty of -3.49 to +6.27%. Larger ranges and slight increases in means are projected for 2050 and 2070. Increases are larger for summer, autumn, and spring compared with winter.

**Extreme rainfall:** A distinct low pressure system forms over the Torres Strait /Coral Sea during heavy rainfall events over the Torres Strait region, Cape York and the tropical rainforest region of north Queensland. The pressure, wind and out-going long wave radiation (OLR) anomalies indicate that they are a part of the large-scale circulation during the wet season. Higher temperatures are observed over southern Australia during the heavy rainfall events in northern Australia, an indication of the intense meridional circulation. Heavy rainfall events and strong winds occur particularly during onset and active periods of the monsoon.

**Solar radiation:** Decreases dominate projected changes in solar radiation. The best estimates of annual change in solar radiation by 2030 for A2 and A1FI emission scenarios are -0.31% and -0.43%, with ranges between -1.18% and 0.82% and between -1.39% and 0.81%, respectively. Slightly higher decreases and larger ranges are projected for 2050 and 2070 for the two emission scenarios.

**Relative humidity:** Due to the location in the tropics, relative humidity is constantly high during the year. Changes in relative humidity in the future is projected to be less than 1% ranging between -1 and +1%.

**Wind speed:** Changes to the annual wind speed are also expected to be small. The best estimate for annual wind speed change by 2030 for the A2 emission scenario is +0.34% with a range between -0.95 and 1.72%. For the A1FI emission scenario, the annual change is +0.37% with a range between -1.12 and 2.47%. A very small increase has been projected in annual and seasonal values for 2050 and 2070 for two emission scenarios.

**Potential evaporation:** Overall there is an increase in potential evaporation in the future with the greatest under the A1FI emission scenario. The best estimate of annual increase by 2030 for the A2 emission scenario is 2.63% with an uncertainty range between 1.94 and 4.72%. For the A1FI emission scenario, the annual increase by 2030 is 3.74% with an uncertainty range between 2.28 and 5.87%. Larger increases and ranges are projected for 2050 and 2070.

## 5.2 Potential climate change impacts in the Torres Strait region

The projected changes show that there is little room for complacency when dealing with potential impacts on various sectors, despite their large uncertainty. The impact of

climate change would increase in severity beyond any stabilisation in atmospheric greenhouse gas concentrations.

Sea level rise due to climate change is one of the biggest threats to the life of communities as most of the islands are close to sea level. The observed sea level rise is 6 mm per year, which is based on satellite measurements between 1993 and 2010. Moreover, this estimate is twice the global value of 3 mm per year. Changes in global sea level is nonlinear and projected to be 0.8 m by 2100. There is still great uncertainty associated with the expected scale and timing of rises in sea level due to the highly dynamic nature of major ice sheets. Current warming of the oceans and atmosphere is likely to drive an increase in global sea level for at least several centuries, even if we drastically reduce the present greenhouse gases emissions.

### **5.3 Conclusions and recommendations**

- Simulated changes in climate indicate that a significant degree of climate change in the Torres Strait region is inevitable, and is likely to become increasingly apparent over the next 30-100 years. Changes are expected in both the mean values and in the magnitudes and frequency of extremes. This means that long-term planning should not assume that future climate and resources will be as they were over the past 100 years. Significant adaptation to a changing climate will be required.
- Characteristics of water quality, flooding areas and storm surges could change significantly, if monsoonal winds in summer and south-easterlies in winter were to become stronger under enhanced greenhouse conditions. Anticipated changes have significant implications for the sustainable development of existing and planned coastal infrastructure.
- Changes in apparent temperature could have increasing impacts on human populations of the region. These changes would affect daily life and the economic livelihood of inhabitants in the region. Significant changes in management and behaviour may be required for adaptation strategies to ensure sustainability.
- ENSO-related climate change at decadal and century scales is expected to affect the region. Some flora and fauna species may come under increasing stress, causing long-term irreversible change in species distribution and composition.
- Significant uncertainties remain in relation to the estimation of future climate. These can be reduced by (1) improving the atmospheric and oceanic forcings input to transient experiments (2) improving the ability of global climate models to simulate ENSO behaviour under present and enhanced greenhouse conditions and (3) improving the high-resolution modelling of the region to better incorporate the effects of topography and air-sea interaction processes. Some of the improvements are, and will be, included in the IPCC AR5 simulations.

- Climate impact and adaptation assessment should be improved by further development of versatile climate impact and adaptation models and methodologies for a number of key sectors and activities. These models should be developed and tested against observations initially. They can then be used to assess the impacts of more-reliable climate change projections with reduced uncertainty when they become available.

## 6. KNOWLEDGE GAPS

**Lack of high-quality data:** A lack of high-quality data sets for the Torres Strait region is a major problem to understand the present climate variability. Rainfall data are available at a number of stations, but observations at many stations have been discontinued. Temperature measurements are available at a handful of stations only. They are maintained by the Australian Bureau of Meteorology. Locations of temperature stations have been changed and recent data are not checked for errors. A set of high-quality air temperature, rainfall and other climate variables is needed to understand the present climate, which could be used as basis for validating climate model simulations before producing any projections.

**ENSO:** ENSO has a strong influence on the climate of the region as shown in section 1.1.6. Although there is a strong link between ENSO and the climate of the region, there is no overarching consensus regarding changes in ENSO dynamics under enhanced greenhouse conditions. In particular, projected changes in the frequency and amplitude of ENSO are ambiguous. ENSO is linked to several large-scale climate drivers that influence both land and oceanic environments. Uncertainty associated with ENSO will also increase uncertainty in the dynamics of other climate drivers, (e.g. Indian Ocean Dipole), tropical cyclones and natural and anthropogenic aerosols.

**Tropical cyclones:** There is large uncertainty about changes to tropical cyclone behaviour due to enhanced greenhouse conditions. Coarse-resolution models fail to simulate tropical cyclones. Higher-resolution models do simulate tropical cyclones, but inherit many deficiencies from global climate models as their boundary conditions are from global climate models. Further research including high-resolution modelling is needed to better understand the likely changes in frequency and intensity of tropical cyclones in the region.

**Climate Change Projections from GCMs:** Global climate models capture primary and most secondary large-scale circulation patterns, but regional to local scale circulation and rainfall patterns are not adequately resolved. This is a crucial factor that affects the Torres Strait region. These models have coarse resolution to resolve circulation patterns where impacts are expected to be important. Large uncertainty is associated with simulations from these models as they do not capture important characteristics of climate drivers of the Torres Strait region such as ENSO, monsoon, South Pacific Convergence Zone (SPCZ), circulation patterns that produce extreme rainfall events, etc. Although the GCMs have coarse resolution, it should be noted that for islands with low topography (e.g. coral cays) the scale of the GCMs is probably of secondary importance than their representation of ENSO and climate drivers. In addition, in terms of getting better high-resolution projections, the need for quality observational data to allow statistical downscaling from GCM data is perhaps another important issue.

**High-resolution regional climate models:** High-resolution grids are one of the best model characteristics likely to get reliable regional and local scale climate information. Simulations from high-resolution models are able to give detail information in topographically complex terrain, such as the rainforest region of northeast Queensland, south-eastern Australia and Tasmania. These simulations usually give higher temporal

resolution data for the region. However, boundary conditions for these models are provided by global climate models which have deficiencies of simulating some important climate drivers. For example, ENSO, South Pacific Convergence Zone (SPCZ), some important features of the monsoon are not readily captured by coarse-resolution global climate models. Higher-resolution global climate models, with improved physical parameterisations, is one of the priorities for better climate change projections made in the future for the region. In recent years, sea surface temperature biases in the global climate models are corrected and used as boundary conditions for the high resolution simulations. These high resolution simulations give better representation of the climate and extremes.

## 7. REFERENCES

- Briggs, G. 2010. The impact of climate change on the Torres Strait and Australia's Indian Ocean territories. Strategic analysis paper, Independent Strategic Analysis of Australia's Global Interests, March 2010, 7p.
- CSIRO and Australian Bureau of Meteorology, 2007: *Climate change in Australia*. Technical Report, 140 pp, <http://www.climatechangeinaustralia.com.au/resources.php>.
- Davidson, N. E. 1984: Short-term fluctuations in the Australian monsoon during winter MONEX. *Monthly Weather Review*, **112**, 1697-1708.
- Folland, C. K., Renwick, J. A., Salinger, J. M. and Mullan, A. B. 2002: Relative influences of the Interdecadal Pacific Oscillation and ENSO on the South Pacific Convergence Zone. *Geophysical Research Letters*, **29**, 1643, 10.1029/2002GL014201.
- Green, D., Alexander, L., McInnes, K., Church, J., Nicholls, N. and White, N. 2010. An assessment of climate change impacts and adaptation for the Torres Strait Islands, Australia. *Climatic Change*, **102**, 405-433.
- Hastings, P. A. 1990: Southern oscillation influences on tropical cyclone activity in the Australian/southwest Pacific region. *International Journal of Climatology*, **10**, 291-298.
- Hendon, H. H. and Liebmann, B. 1990: A composite study of onset of the Australian summer monsoon. *Journal of the Atmospheric Sciences*, **47**, 2227-2240.
- IPCC, 2007: *Climate Change 2007: The Physical Science – Summary for Policymakers*. Contribution of Working Group I to the Fourth Assessment Report of the Intergovernmental Panel on Climate Change, 17pp.
- Johnson, J. E. and Marshall, P. A. 2007: Climate change and the Great Barrier Reef. A Vulnerability Assessment. Great Barrier Reef Marine Park Authority and Australian Greenhouse Office, Australia.
- Keenan, T. D. and Brody, L. R. 1988: Synoptic scale modulation of convection during the Australian summer monsoon. *Monthly Weather Review*, **116**, 71-85.
- Knutson, T. R., McBride, J. L., Chan, J., Emanuel, K., Holland, G., Landsea, C., Held, I., Kossin, J. P., Srivastava, A. K. and Sugi, M. 2010: Tropical cyclones and climate change. *Nature Geoscience*, **21**, 157-163.
- Lough, J. 2007: Climate and climate change on the Great Barrier Reef. In: *Climate change and the Great Barrier Reef*, Eds Johnson, J. E. and Marshall, P. A., Great Barrier Reef Marine Park Authority and Australian Greenhouse Office, Australia, 16-50.

- Love, G. 1985: Cross-equatorial influence of winter hemisphere subtropical cold surges. *Monthly Weather Review*, **113**, 1487-1498.
- Madden, R. A. and Julian, P. R. 1971: Detection of a 40-50 day oscillation in the zonal wind in the tropical Pacific. *Journal of the Atmospheric Sciences*, **28**, 702-708.
- Manins, P, Allan, R., Beer, T., Fraser, P., Holper, P., Suppiah, R. and Walsh, K. 2001: *Atmosphere*. Australia State of the Environment report 2001, (Theme Report). CSIRO Publishing on behalf of the Department of Environment and Heritage, Canberra.
- Mantua, N. J. and Hare. S. R. 2002: The Pacific decadal oscillation. *Journal of Oceanography*, **58**, 35-44.
- McBride, J. L. 1987: The Australian monsoon. In: Monsoon Meteorology, C. P Chang and T. N. Krishnamurti, Eds., Oxford University Press, 203-231.
- McBride, J. L. and Keenan, T. D. 1982: Climatology of tropical cyclone genesis in the Australian region. *International Journal of Climatology*, **2**, 13-33.
- McBride, J. L. and Nicholls, N. 1983: Seasonal relationships between Australian rainfall and the southern oscillation. *Monthly Weather Review*, **111**, 1998-2004.
- Meehl, G. A., Covey, C., Delworth, T., Latif, M., McAvaney, B., Mitchell, J.F.B., Stouffer R.J. and Taylor, K.E. 2007a: The WCRP CMIP3 multimodel dataset: A new era in climate change research. *Bulletin of the American Meteorological Society*, **88**, 1383–1394.
- Meehl, G.A., Stocker, T.F., Collins, W.D., Friedlingstein, P., Gaye, A.T., Gregory, J.M., Kitoh, A., Knutti, R., Murphy, J.M., Noda, A., Raper, S.C.B., Watterson, I.G., Weaver A.J. and Zhao, Z.-C. 2007b: *Global Climate Projections*. In: *Climate Change 2007: The Physical Science Basis*. Contribution of Working Group I to the Fourth Assessment Report of the Intergovernmental Panel on Climate Change, Eds., Solomon, S., Qin, D., Manning, M., Chen, Z., Marquis, M., Averyt, K.B., Tignor, M. and Miller, H.L., Cambridge University Press, Cambridge, United Kingdom and New York, NY, USA.
- Mitchell, T. D. 2003: Pattern scaling: An examination of the accuracy of the technique for describing future climates. *Climatic Change*, **60**, 217-242.
- Mitchell, J. F. B., Johns, T. C., Eagles, M., Ingram, W. J., and Davis, R. A.1999: Towards the construction of climate change scenarios. *Climatic Change*, **41**, 547-581.
- Mitchum, G. T., Nerem, R. S., Merrifield, M. A. and Gehrels, W. R. 2010: Model sea level change estimates. In: *Understanding sea-level rise and variability*, Eds. J. A. Church, P. L. Woodworth, T. Aarup and W. S. Wilson, Wiley-Blackwell, Chichester, UK, 122-142.
- Nakićenović, N., and Swart, R. (Eds.), 2000: *Special Report on Emissions Scenarios*. A Special Report of Working Group III of the Intergovernmental Panel on Climate Change, Cambridge University Press, Cambridge, United Kingdom and New York, NY, USA, 599 pp.

- Parnell, K. E. and Smithers, S. G. 2010: Cay island dynamics in Torres Strait: the science information community decisions. MTSRF Annual Conference 2010, Cairns.
- Power, S., F. Tseitkin, V. Metha, B. Lavery, S. Torok and Holbrook, N. 1999: Decadal climate variability in Australia during the twentieth century. *International Journal of Climatology*, **19**, 169-184.
- Reisinger, A., Meinshausen, M., Manning, M. and Bodeker, G. 2010: Uncertainties of global warming metrics: CO<sub>2</sub> and CH<sub>4</sub>. *Geophysical Research Letters*, **37**, L14707, doi:10.1029/2010GL043803, 1-6.
- Salinger, M. J., Renwick, J. A. and Mullan, A. B. 2001: Interdecadal Pacific Oscillation and south Pacific climate. *International Journal of Climatology*, **21**, 1705-1721.
- Smith, I. N., Wilson, L. and Suppiah, R. 2008: Characteristics of the northern Australian rainy season. *Journal of Climate*, **21**, 4298-4311.
- Smith, I. and Chandler, E. 2010: Refining rainfall projections for the Murray Darling basin of south-east Australia – the effect of sampling model results based on performance. *Climatic Change*, **102**, 377-393.
- Solomon, , S., Qin, D., Manning, M., Chen, Z., Marquis, M., Averyt, K., Tignor, M. and Miller, M. 2007: Climate change 2007: the physical science basis. Contribution of working group I to the fourth assessment report of the intergovernmental panel on climate change. Cambridge University Press, Cambridge.
- Steadman, R. G. 1984: A universal scale of apparent temperature. *Journal of Applied Meteorology*, **23**, 1674-1687.
- Steadman, R. G. 1994: Norms of apparent temperature in Australia. *Australian Meteorological Magazine*, **23**, 1-16.
- Suppiah, R. 1992: The Australian summer monsoon: A review. *Progress in Physical Geography*, **16**, 283-318.
- Suppiah, R. 1993: ENSO phenomenon and 30-50 day variability in the Australian summer monsoon rainfall. *International Journal of Climatology*, **13**, 837-51 .
- Suppiah, R. and Wu, X. 1998: Surges, cross-equatorial flows and their links with the Australian summer monsoon circulation and rainfall. *Australian Meteorological Magazine*, **47**, 113-130.
- Suppiah, R., Hennessy, K. J., Whetton, P. H., McInnes, K., Macadam, I., Bathols, J., Ricketts, J. and Page, C. M. 2007: Australian climate change projections derived from simulations performed for the IPCC 4<sup>th</sup> Assessment report. *Australian Meteorological Magazine*, **56**, 131-152.
- TSRA. 2010: Torres Strait Climate Change Strategy. Report prepared by the Land and Sea Management Unit, Torres Strait regional Authority, May 2010, 20p.

- Watterson, I.G., 2008: Calculation of probability density functions for temperature and precipitation change under global warming. *Journal of Geophysical Research*, **113**, D12106, doi:10.1029/2007JD009254.
- Webster, P. J. 1981: Cold surges of the winter monsoon: dynamic structures. *Proceedings of the International Conference of the Scientific Results of the Monsoon Experiments*, Denpasar, Indonesia, WMO, 2-3 to 2-8.
- Whalan, S, 2009: Ecological role and potential economic value of sponges to the Torres Strait: Annual Report2009. Report to the Marine and Tropical Sciences Research Facility. Reef and Rainforest Research Centre Limited, Cairns, 45p.
- Wheeler, M. C. and J. L. McBride. 2005: Australia-Indonesian monsoon. In W.K. M. Lau and D. E. Waliser (eds), *Intraseasonal Variability in the Atmosphere-Ocean Climate System*, Praxis Publishing Ltd, Chichester, UK, 125-174.
- Whetton, P. H., McInnes, K. L., Jones, R. N., Hennessy, K. J., Suppiah, R., Page, C. M., Bathols, J. and Durack, P. J. 2005: *Australian climate change projections for impact assessment and policy application : A Review.*, CSIRO, Marine and Atmospheric Research Paper 001, Aspendale, 34pp





